

Lecture Notes by Jürgen Vollmer

Theoretical Mechanics

— Working Copy — Chapter 6 —

— 2022-02-05 05:50:55+01:00—

Copyright © 2020 Jürgen Vollmer

LECTURES DELIVERED AT FAKULTÄT FÜR PHYSIK UND GEOWISSENSCHAFTEN, UNIVERSITÄT LEIPZIG
<http://www.uni-leipzig.de/physik/~vollmer>

Contents

Table of Contents v

Preface v

1	<i>Basic Principles</i>	1
1.1	<i>Basic notions of mechanics</i>	2
1.2	<i>Dimensional analysis</i>	6
1.3	<i>Order-of-magnitude guesses</i>	9
1.4	<i>Problems</i>	10
1.5	<i>Further reading</i>	12
2	<i>Balancing Forces and Torques</i>	13
2.1	<i>Motivation and outline: forces are vectors</i>	14
2.2	<i>Sets</i>	15
2.3	<i>Groups</i>	21
2.4	<i>Fields</i>	24
2.5	<i>Vector spaces</i>	27
2.6	<i>Physics application: balancing forces</i>	32
2.7	<i>The inner product</i>	34
2.8	<i>Cartesian coordinates</i>	36
2.9	<i>Cross products — torques</i>	41
2.10	<i>Worked example: Calder's mobiles</i>	48
2.11	<i>Problems</i>	49
2.12	<i>Further reading</i>	58

3	<i>Newton's Laws</i>	59
3.1	<i>Motivation and outline: What is causing motion?</i>	60
3.2	<i>Time derivatives of vectors</i>	60
3.3	<i>Newton's axioms and equations of motion (EOM)</i>	62
3.4	<i>Constants of motion (CM)</i>	70
3.5	<i>Worked example: Flight of an Earth-bound rocket</i>	80
3.6	<i>Problems</i>	83
3.7	<i>Further reading</i>	90
4	<i>Motion of Point Particles</i>	91
4.1	<i>Motivation and outline: EOM are ODEs</i>	92
4.2	<i>Integrating ODEs — Free flight</i>	94
4.3	<i>Separation of variables — Settling with Stokes drag</i>	98
4.4	<i>Worked example: Free flight with turbulent friction</i>	105
4.5	<i>Linear ODEs — Particle suspended from a spring</i>	108
4.6	<i>The center of mass (CM) inertial frame</i>	115
4.7	<i>Worked example: the Kepler problem</i>	120
4.8	<i>Mechanical similarity — Kepler's 3rd Law</i>	121
4.9	<i>Solving ODEs by coordinate transformations — Kepler's 1st law</i>	122
4.10	<i>Problems</i>	126
4.11	<i>Further reading</i>	133
5	<i>Impact of Spatial Extension</i>	135
5.1	<i>Motivation and outline: How do particles collide?</i>	136
5.2	<i>Collisions of hard-ball particles</i>	138
5.3	<i>Volume integrals — A professor falling through Earth</i>	140
5.4	<i>Center of mass and spin of extended objects</i>	147
5.5	<i>Bodies with internal degrees of freedom: Revisiting mobiles</i>	152
5.6	<i>Worked example: Reflection of balls</i>	157
5.7	<i>Problems</i>	158
6	<i>Integrable Dynamics</i>	161
6.1	<i>Motivation and Outline: How to deal with constraint motion?</i>	162
6.2	<i>Lagrange formalism</i>	164

<i>h one degree of freedom</i>	174
6.4 <i>Dynamics with two degrees of freedom</i>	186
6.5 <i>Dynamics of 2-particle systems</i>	190
6.6 <i>Conservation laws, symmetries, and the Lagrange formalism</i>	190
6.7 <i>Worked problems: spinning top and running wheel</i>	190
6.8 <i>Problems</i>	190
7 <i>Deterministic Chaos</i>	189
<i>Take Home Messags</i>	191
A <i>Physical constants, material constants, and estimates</i>	193
A.1 <i>Solar System</i>	193
<i>Bibliography</i>	195

6

Integrable Dynamics

In Chapter 5 we considered objects that consist of a mass points with fixed relative positions, like a flying and spinning ping-pong ball. Rather than providing a description of each individual mass element, we established equations of motion for their center of mass and the orientation of the body in space. From the perspective of theoretical mechanics the fixing of relative positions is a constraint to their motion, just as the ropes of a swing enforces a motion on a one-dimensional circular track, rather than in two dimensions. The deflection angle θ of the pendulum, and the center of mass and orientation of the ball are examples of generalized coordinates that automatically take into account the constraints.

In this chapter we discuss how to set up generalized coordinates and how to find the associated equations of motion. The discussion will be driven by examples. The examples will be derived from the realm of integrable dynamics. These are systems where conservation laws can be used to break down the dynamics into separate problems that can be interpreted as motion with a single degree of freedom.

At the end of the chapter you know why coins run away rolling on their edge, and how the speed of a steam engine was controlled by a mechanical device. Systems where the dynamics is not integrable will subsequently be addressed in Chapter 7.



Marguerite Martyn, 1914
wikimedia/public domain

Figure 6.1: The point-particle idealization of a girl on a swing is the mathematical pendulum of Figures 1.2 and 1.3.

add more pics

6.1 Motivation and Outline:

How to deal with constraint motion?

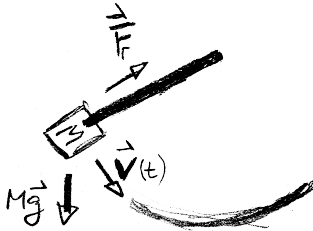


Figure 6.2: Forces acting for the motion of a swing, or its equivalent idealization of a mathematical pendulum.

Almost all interesting problems in mechanics involve constraints due to rails or tracks, and due to mechanical joints of particles. The most elementary example is a swing (Figure 6.1), where a rope forces a mass M to move on a path with positions constrained to a circle with radius given by the length L of the rope. Gravity Mg and the pulling force F_r of the rope acting act on the mass (Figure 6.2). However, how large is the latter force? At the topmost point of its trajectory the mass is at rest, and no force is needed along the rope to keep it on its track. At the lowermost point, where the swing goes with its maximum speed, there is a substantial force. Newton's formalism requires a discussion of these forces. Lagrange established an alternative approach that provides equations of motion with substantially less effort. The key idea of this formalism is to select generalized coordinates adapted to the problem.

Definition 6.1: Generalized Coordinates

We consider N particles moving in D dimensions. There are forces that keep the particles on a subset of space with a dimension smaller than D , and their relative positions may be constrained by bars and joints. Due to the constraints the system only has $M < DN$ degrees of freedom. In this chapter we denote the positions of the particles as $\mathbf{x} \in \mathbb{R}^{DN}$, and we specify position compatible with the constraints as $\mathbf{x}(\mathbf{q}(t))$, where $\mathbf{q} \in \mathbb{R}^M$ are the *generalized coordinates* adapted to the constrained motion.

Example 6.1: Generalized coordinates for a pendulum

We describe the position of the mass in a mathematical pendulum by the angle $\theta(t)$, as introduced in Example 1.10. The position of the mass in the 2D pendulum plane is thus described by the vector

$$\mathbf{x}(t) = L \begin{pmatrix} \sin \theta(t) \\ -\cos \theta(t) \end{pmatrix} = L \hat{\mathbf{R}}(\theta(t)).$$

In view of the chain rule its velocity amounts to

$$\dot{\mathbf{x}} = L \dot{\theta} \partial_{\theta} \hat{\mathbf{R}}(\theta(t)) = L \dot{\theta} \hat{\boldsymbol{\theta}}(\theta(t)) \quad \text{with} \quad \hat{\boldsymbol{\theta}}(\theta(t)) = \begin{pmatrix} \cos \theta(t) \\ \sin \theta(t) \end{pmatrix}$$

Remark 6.1. Note that $\hat{\mathbf{R}}(\theta)$ and $\hat{\boldsymbol{\theta}}(\theta)$ are orthonormal vectors that describe the position of the mass in terms of polar coordinates rather than fixed-in-space Cartesian coordinates. □

Theorem 6.1: Basis vectors for polar coordinates


Let $\{\hat{x}, \hat{z}\}$ be a basis of \mathbb{R}^2 , and (R, θ) be the polar coordinates¹ associated to a point with Cartesian coordinates (x, z) . Then


- $R = \sqrt{x^2 + z^2}$ is the distance of the point from the origin
- $\theta = -\arctan(x/z)$ the angle with respect to $-\hat{z}$,

We denote the vector from the origin to (R, θ) as $R \hat{R}(\theta)$. Then the following statements hold

- $\hat{R}(\theta)$ is a normal vector at the position (R, θ) of a circle C_R with center at the origin at radius R .
- $\hat{\theta} = \partial_\theta \hat{R}$ is a vector tangential to C_R at the position (R, θ) .
- $\partial_\theta \hat{\theta} = -\hat{R}$.
- For every $\theta \in [0, 2\pi)$ the vectors $\{\hat{R}(\theta), \hat{\theta}(\theta)\}$ form an orthonormal basis of \mathbb{R}^2 .

¹ The choice of the axes and the angle reflects the notations adopted in Figures 1.2 and 1.3.

Remark 6.2. The coordinate representation of $\hat{R}(\theta)$ and $\hat{\theta}(\theta)$ in Cartesian coordinates is provided in Example 6.1. 

Remark 6.3. The assertions of Theorem 6.1 also apply when the unit vectors of \mathbb{R}^2 are denoted as $\{\hat{x}, \hat{y}\}$, and when the angle θ denotes the angle with respect of the \hat{x} axis. The different reference axis *only* changes the coordinate representation of the vectors. 

Example 6.2: Generalized coordinates for a ping-pong ball

A ping-pong ball consists of N atoms located in the three-dimensional space. During a match they follow an intricate trail in the vicinity of the ping-pong players. At any time during their motion the atoms are located on a thin spherical shell with fixed positions with respect to each other. Rather than specifying the position of each atom one can therefore specify the position of the ball in terms of six generalized coordinates (Figure 6.3): Three coordinates provide its center of mass. The orientation of the ball can be provided by specifying the orientation of a body fixed axis in terms of its polar and azimuthal angle, and a third angle specifies the orientation of a point on its equator when rotating the ball around the axis.

Generalized coordinates describe only positions complying with the constraints of the motion, and they do not account for other positions from the very beginning. Lagrange's key observation is that constraint forces, e.g. the force on the rope of the swing, only act in a direction orthogonal to the positions described by generalized coordinates. Therefore, the constraint forces do not affect the time evolution of generalized coordinates. For the pendulum and the

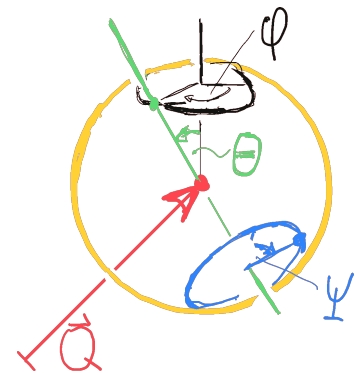


Figure 6.3: The position of a ball in space can be described in terms of a 3D vector Q that describes the center of the ball (red dot), angles θ, ϕ that describe the orientation in space of a fixed axis in the ball (green line), and another angle ψ that describes the position of point that is not on the axis (blue point).

ping-pong ball one only has to account for gravity to find the evolution of the generalized coordinates. There is no need to deal with the force along the rope in the swing, and the atomic interaction forces that keep atoms in their positions in the ping-pong ball.

Outline

In Section 6.2 we will introduce the Lagrange formalism that will allow us without much ado to determine the EOM for generalized coordinates. Subsequently, in Section 6.3 we deal with systems with a single degree of freedom. In Section 6.4 we will see how symmetries in the dynamics allow us to eliminate a second degree of freedom based on an informed choice of generalized coordinates. Section 6.5 deals with two-particle systems and other problems where one deals with several degrees of freedom. In all cases we will eventually reduce the dynamics to one-dimensional problems. The final Section 6.6 deals with the relation between continuous symmetries of the dynamics and conservation laws.

6.1.1 Self Test

Problem 6.1. Different reference axes for polar coordinates

Verify the assertions of Theorem 6.1 and Remark 6.3:

- a) Specify the coordinate representation of $\{\hat{\mathbf{R}}(\theta), \hat{\boldsymbol{\theta}}(\theta)\}$ for the case where θ denotes the angle with respect to the positive \hat{x} axis.
- b) Verify the assertion of Theorem 6.1.

Problem 6.2. Describing the orientation of dice

We place a die on the table such that its center lies at the origin of a 3D Cartesian coordinate frame, and its axes are aligned with the coordinate axes. We characterize the configuration of the die by the number of dots on the faces pointing in the three positive coordinate directions.

- a) Show that there are 24 different possibilities to place the die.
- b) Determine the angles (θ, ϕ, ψ) (cf. Figure 6.3) that will turn a die from the configuration be $(1, 2, 3)$ to

$$\text{b}_1) (2, 3, 4) \quad \text{b}_2) (4, 6, 2) \quad \text{b}_3) (1, 3, 5)$$

6.2 Lagrange formalism

The Lagrange formalism provides an effective approach to derive the EOM for generalized coordinates. We first provide a derivation in a Cartesian coordinate frame. Then we discuss how the EOM for generalized coordinates are determined.

6.2.1 Euler-Lagrange equations for Cartesian coordinates

In Section 5.5 we saw that a mobile will be at rest in a position characterized by the coordinate vector \mathbf{x} when the leading order correction $\delta\mathbf{x} \cdot \nabla\Phi(\mathbf{x})$ to its potential energy $\Phi(\mathbf{x})$ vanishes for every perturbation $\delta\mathbf{x}$ of the position. In the following we denote the leading order corrections term of the Taylor expansion as variation.

Definition 6.2: Variation of a scalar function

Let $f : \mathbb{D} \times [t_I, t_E] \rightarrow \mathbb{R}$ with $\mathbb{D} \subset \mathbb{R}^D$ be function that has continuous first derivatives for all $\mathbf{x} \in \mathbb{D}$. The *variation of f* for a small deviation $\delta\mathbf{x}$ of \mathbf{x} such that $\mathbf{x} + \delta\mathbf{x} \in \mathbb{D}$ amounts to the linear-order term of the Taylor expansion of f ,

$$\delta f(\mathbf{x}, t) = \delta\mathbf{x} \cdot \nabla_{\mathbf{x}} f(\mathbf{x}, t) = \sum_{i=1}^D \delta x_i \frac{\partial f(\mathbf{x}, t)}{\partial x_i}$$

In Section 5.5 we showed that $\delta\Phi(\mathbf{x}_0) = 0$ for every critical point \mathbf{x}_0 where the system is (and remains) at rest. We now also account for explicitly time-dependent potentials $\Phi(\mathbf{x}, t)$ and consider the variations $\delta\mathbf{x}(t)$ of time dependent trajectories $\mathbf{x}(t)$ with $t \in [t_I, t_F]$. Here $\delta\mathbf{x}(t)$ describes the deviation of the perturbed trajectory from the reference trajectory $\mathbf{x}(t)$ at time t , and it is understood that $\delta\mathbf{x}(t_I) = \delta\mathbf{x}(t_F) = \mathbf{0}$. Now we have

$$\delta\Phi(\mathbf{x}, t) = \delta\mathbf{x} \cdot \nabla_{\mathbf{x}}\Phi(\mathbf{x}, t) = -\delta\mathbf{x} \cdot \mathbf{F}(\mathbf{x}, t) = -\delta\mathbf{x} \cdot m\ddot{\mathbf{x}}$$

The velocity and acceleration for the perturbed trajectory $\mathbf{x} + \delta\mathbf{x}$ are $\dot{\mathbf{x}} + \delta\dot{\mathbf{x}}$ and $\ddot{\mathbf{x}} + \delta\ddot{\mathbf{x}}$ such that

$$\frac{d}{dt}(m\dot{\mathbf{x}} \cdot \delta\mathbf{x}) = m\ddot{\mathbf{x}} \cdot \delta\mathbf{x} + m\dot{\mathbf{x}} \cdot \delta\dot{\mathbf{x}} = m\ddot{\mathbf{x}} \cdot \delta\mathbf{x} + \delta\frac{m\dot{\mathbf{x}}^2}{2}$$

where $T = m\dot{\mathbf{x}}^2/2$ is the kinetic energy. Hence, we can express the variation of the potential as

$$\begin{aligned} \delta\Phi(\mathbf{x}, t) &= -\frac{d}{dt}(\delta\mathbf{x} \cdot m\dot{\mathbf{x}}) + \delta T(\dot{\mathbf{x}}) \\ \Rightarrow \delta(T(\dot{\mathbf{x}}) - \Phi(\mathbf{x}, t)) &= -\frac{d}{dt}(\delta\mathbf{x} \cdot m\dot{\mathbf{x}}) \end{aligned}$$

The difference between the kinetic and potential energy is a total time derivative. Integrating the expression over time from t_I to t_F therefore provides

$$\int_{t_I}^{t_F} dt \delta(T(\dot{\mathbf{x}}) - \Phi(\mathbf{x}, t)) = -\int_{t_I}^{t_F} dt \frac{d}{dt}(\delta\mathbf{x} \cdot m\dot{\mathbf{x}}) \quad (6.2.1)$$

$$= \delta\mathbf{x}(t_I) \cdot m\dot{\mathbf{x}}(t_I) - \delta\mathbf{x}(t_F) \cdot m\dot{\mathbf{x}}(t_F) = 0 \quad (6.2.2)$$

The integral vanishes because \mathbf{x} is fixed at the start and the end point.

Up to mathematical identities that are always true we only used Newton's law $\mathbf{F}(\mathbf{x}, t) = m\ddot{\mathbf{x}}$ to arrive at this conclusion. This observation is denoted as the principle of least action. Rather than on

Newton axioms we may therefore base mechanics on the principle of least action.

Definition 6.3: Lagrangian

We consider a dynamics with kinetic energy $T(\dot{\mathbf{x}}(t))$ and potential energy $\Phi(\mathbf{x}(t), t)$ for trajectories $\mathbf{x}(t)$. The difference

$$\mathcal{L}(\mathbf{x}, \dot{\mathbf{x}}, t) = T(\dot{\mathbf{x}}) - \Phi(\mathbf{x}, t)$$

will be called *Lagrangian* or *Lagrange function* of the dynamics.

Definition 6.4: Action of a trajectory

For a dynamics with Lagrangian $\mathcal{L}(\mathbf{x}, \dot{\mathbf{x}}, t)$ the *action* $S[\mathbf{x}(t), \dot{\mathbf{x}}(t)]$ of a trajectory $\mathbf{x}(t)$, $t_I \leq t \leq t_F$ with velocity $\dot{\mathbf{x}}(t)$ is defined as

$$S[\mathbf{x}(t), \dot{\mathbf{x}}(t)] = \int_{t_I}^{t_F} dt \mathcal{L}(\mathbf{x}(t), \dot{\mathbf{x}}(t), t) \quad (6.2.3)$$

The *variation of the action* will be defined as

$$\delta S[\mathbf{x}(t), \dot{\mathbf{x}}(t)] = \int_{t_I}^{t_F} dt \delta \mathcal{L}(\mathbf{x}(t), \dot{\mathbf{x}}(t), t)$$

Axiom 6.1: Principle of least action

Let $\mathbf{x}(t)$ with $t_I \leq t \leq t_F$ be a trajectory from $\mathbf{x}(t_I)$ to $\mathbf{x}(t_F)$ that satisfies Newton's law $F(\mathbf{x}, t) = m\ddot{\mathbf{x}}$ with a force that is derived from a potential $\Phi(\mathbf{x}, t)$. Then the variation of the action associated the trajectory will vanish

$$0 = \delta S[\mathbf{x}(t), \dot{\mathbf{x}}(t)]$$

Remark 6.4. The principle is called the principle of *least* action. However, it only requires that the action has a critical point. There are many examples in physics where the action takes a saddle point, rather than a minimum. □

The principle provides an alternative way to determine the EOM that proceeds as follows.

$$\begin{aligned} 0 = \delta S[\mathbf{x}(t), \dot{\mathbf{x}}(t)] &= \int_{t_I}^{t_F} dt \delta \mathcal{L}(\mathbf{x}(t), \dot{\mathbf{x}}(t), t) \\ &= \int_{t_I}^{t_F} dt [\delta \dot{\mathbf{x}} \nabla_{\dot{\mathbf{x}}} \mathcal{L}(\mathbf{x}, \dot{\mathbf{x}}, t) + \delta \mathbf{x} \nabla_{\mathbf{x}} \mathcal{L}(\mathbf{x}, \dot{\mathbf{x}}, t)] \\ &= \int_{t_I}^{t_F} dt \delta \mathbf{x} \left[\left(-\frac{d}{dt} \nabla_{\dot{\mathbf{x}}} \mathcal{L}(\mathbf{x}, \dot{\mathbf{x}}, t) \right) + \nabla_{\mathbf{x}} \mathcal{L}(\mathbf{x}, \dot{\mathbf{x}}, t) \right] \end{aligned}$$

² The boundary term of the partial integration vanishes,

$$\begin{aligned} [\delta \mathbf{x} \nabla_{\dot{\mathbf{x}}} \mathcal{L}(\mathbf{x}, \dot{\mathbf{x}}, t)]_{t_I}^{t_F} &= \delta \mathbf{x}(t_F) [\nabla_{\dot{\mathbf{x}}} \mathcal{L}(\mathbf{x}, \dot{\mathbf{x}}, t)]_{t=t_F} \\ &\quad - \delta \mathbf{x}(t_I) [\nabla_{\dot{\mathbf{x}}} \mathcal{L}(\mathbf{x}, \dot{\mathbf{x}}, t)]_{t=t_F} \\ &= 0 \end{aligned}$$

In the last step we performed a partial integration.² The integral must vanish for every choice of the variation $\delta \mathbf{x}$. In particular we may choose a function $\delta \mathbf{x}$ that takes the same sign as the square bracket whenever it does not vanish. However, in that case the

integral is strictly positive unless the square bracket vanishes. This provides the EOM of the dynamics in terms of the Euler-Lagrange equation.

Theorem 6.2: Euler-Lagrange equations

Let $x_i(t)$ be a coordinates of a trajectory $x(t)$ of a dynamics with Lagrangian $\mathcal{L}(x, \dot{x}, t)$. Then $x_i(t)$ is a solution of the Euler-Lagrange equation

$$\frac{d}{dt} \frac{\partial}{\partial \dot{x}_i} \mathcal{L}(x, \dot{x}, t) = \frac{\partial}{\partial x_i} \mathcal{L}(x, \dot{x}, t) \quad (6.2.4)$$

6.2.2 *Mathematical background: variational calculus*

The principle of least action is an application of variational calculus to the action integral, Equation (6.2.3). In order to provide a better intuition of the mathematical concept of the variation, we demonstrate now how one can derive a differential equation of the shortest path on a plane.

Shortest path in a 2d plane. We describe a curve from the origin, $(0, 0)$ to the position (x_e, y_e) in the plane by a function $f(x)$ with $f(0) = 0$ and $f(x_e) = y_e$. Hence, the curve follows the coordinates $q = (x, f(x))$, and according to Remark 3.7 the length of a curve is determined by the line integral

$$L[f(x)] = \int_0^{x_e} dx \mathcal{D}_{\text{plane}}(f(x), f'(x))$$

$$\text{with } \mathcal{D}_{\text{plane}}(f(x), f'(x)) = \left| \frac{dq}{dx} \right| = \sqrt{1 + (f'(x))^2}$$

where $f'(x) = df(x)/dx$. Paths of minimal length must therefore be solutions of the Euler-Lagrange equation

$$0 = \frac{\partial \mathcal{D}}{\partial f} = \frac{d}{dx} \frac{\partial \mathcal{D}}{\partial f'} = \frac{d}{dx} \frac{f'(x)}{\sqrt{1 + (f'(x))^2}}$$

which implies that there is a constant K with

$$\begin{aligned} K &= \frac{f'(x)}{\sqrt{1 + (f'(x))^2}} \Rightarrow K^2 (1 + (f'(x))^2) = (f'(x))^2 \\ &\Rightarrow f'(x) = \frac{K}{\sqrt{1 - K^2}} = \text{const} \end{aligned}$$

Consequently, the shortest connection between two points in the plane is a straight line, where the slope is constant. We urge the reader to go through the steps of the derivation of the Euler-Lagrange equation for this problem, and to take note of the important requirement that the variation of the path δq must vanish at *both* endpoints of the trajectory. An example of a variational problem where this requirement is relaxed is provided in Problem 6.4.

Shortest path on a cylinder surface. We describe a curve on a cylinder with radius R by adopting cylinder coordinates and specifying $z(\theta)$ for the range $\mathcal{I} = [\theta_I, \theta_E]$. The values at the boundary of \mathcal{I} will be denoted as $z(\theta_I) = z_I$ and $z(\theta_E) = z_E$. Hence, the curve follows the coordinates $\mathbf{q} = z(\theta) \hat{z} + R \hat{r}(\theta)$ along a path with direction

$$\mathbf{q}'(\theta) = \frac{d\mathbf{q}}{d\theta} = z'(\theta) \hat{z} + R \hat{\theta}(\theta)$$

The length of this curve is determined by the line integral

$$L[z(\theta)] = \int_{\theta_I}^{\theta_E} d\theta \mathcal{D}_{\text{cyl}}(z(\theta), z'(\theta))$$

$$\text{with } \mathcal{D}_{\text{cyl}}(z(\theta), z'(\theta)) = \left| \frac{d\mathbf{q}}{d\theta} \right| = R \sqrt{1 + (z'(\theta)/R)^2}$$

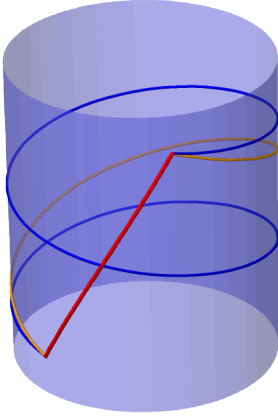


Figure 6.4: Paths of extremal length on a cylinder. In this pictures we have $\theta_E - \theta_I = \pi/3$, $h_E - h_I = 3R$, and we show paths with winding numbers $n \in \{0, -1, -2\}$.

The distance function \mathcal{D}_{cyl} of this problem is identical to the one for the plane, up to replacing $f(x)$ by $z(\theta)$ and x by $R\theta$. Hence, the solutions will be paths of the form

$$z(\theta) = z_I + \frac{z_E - z_I}{\theta_E - \theta_I + 2\pi n} (\theta - \theta_I) \quad \text{with } n \in \mathbb{Z}$$

When one makes sure that $\theta_E \in (\theta_I - \pi, \theta_I + \pi)$ then the solution for $n = 0$ represents the shortest path from z_I to z_E . For $\theta_E - \theta_I = \pi$ the path for $n = 0$ and $n = -1$ have the same length. All other paths represent local minima of L . Small perturbations of the path will increase the length. However, trajectories that reach the final point with a smaller number of loops around the cylinder will in general be shorter. An example is shown in Figure 6.4.

Shortest path on a catenoid. A catenoid is the surface of revolution of the hyperbolic cosine function. We describe a curve on a catenoid with radius $\cosh z$ at height z by adopting cylinder coordinates and specifying $\theta(z)$ for the range $\mathcal{I} = [z_I, z_E]$.³ The values at the boundary of \mathcal{I} are now denoted as $z(\theta_I) = z_I$ and $z(\theta_E) = z_E$. Hence, the curve follows the coordinates $\mathbf{q} = z \hat{z} + \cosh z \hat{r}(\theta(z))$ along a path with direction

$$\mathbf{q}'(z) = \frac{d\mathbf{q}}{dz} = \hat{z} + \sinh z(\theta) \hat{r}(\theta(z)) + \cosh z(\theta) z'(\theta) \hat{\theta}(\theta(z))$$

The length of this curve is determined by the line integral

$$L[z(\theta)] = \int_{z_I}^{z_E} dz \mathcal{D}_{\text{cat}}(\theta(z), \theta'(z))$$

$$\text{with } \mathcal{D}_{\text{cat}}(\theta(z), \theta'(z)) = \left| \frac{d\mathbf{q}}{dz} \right| = \sqrt{(1 + \theta'(z)^2) \cosh^2 z + \sinh^2 z}$$

Consequently, the Euler-Lagrange function takes the form

$$0 = \frac{\partial \mathcal{D}_{\text{cat}}}{\partial \theta} = \frac{d}{dz} \frac{\partial \mathcal{D}_{\text{cat}}}{\partial \theta'} = \frac{d}{dz} \frac{\theta'(z) \cosh^2 z}{\sqrt{(1 + \theta'(z)^2) \cosh^2 z + \sinh^2 z}}$$

³ The surface is no longer translation invariant along the axis, but still rotation symmetric. As a consequence, $\theta(z)$ will turn out to be a cyclic variable, while a parameterization in terms of $z(\theta)$ will involve nontrivial derivatives with respect to z . You may check this in Problem 6.3.

The variable θ is cyclic and we denote the entailed conservation law as K . Rearranging terms provides

$$\theta'(z) = K \sqrt{\frac{1 + \tanh^2 z}{\cosh^2 z - K^2}}$$

such that

$$\theta(z) = \theta_I + K \int_{z_I}^z dz \sqrt{\frac{1 + \tanh^2 z}{\cosh^2 z - K^2}}$$

The shortest paths on the catenoid must be determined by numerical evaluation of this integral.

make fig with paths on catenoid

Problem 6.5 extends the present discussion to situations where one minimizes the surface *area* of a soap film, rather than a feature of a one-dimensional object. Problem 6.11 addresses extremal paths on a sphere. Unless two points lie exactly on opposite sides of the sphere (like North and South pole) there are exactly two trajectories of extremal length. One of them is the shortest trajectory. The other one is a saddle point.

6.2.3 Euler-Lagrange equations for generalized coordinates

The Euler-Lagrange equations derive from a variational principle stating that the gradient of the Lagrange function with respect to the phase-space coordinate $\Gamma = (x, \dot{x})$ must vanish for physically admissible trajectories. This holds for *all* directions in phase space. However, generalized coordinates do not qualify as a vector such that some care is needed to derive their EOM.

Example 6.3: Rollercoaster trail

The position $x(t)$ on the trail of a rollercoaster can uniquely be described by the (dimensionless) distance ℓ along the trail that it has gone. Hence, generalized coordinate $\ell(t)$ uniquely describes the configuration $x(\ell(t))$ of the rollercoaster at time t .

Example 6.4: Driven pendulum

A driven pendulum is a mathematical pendulum where the position of the fulcrum X_f and the length of the pendulum arm $L(t)$ are subjected to a prescribed temporal evolution. The position of the pendulum weight, x , may then be described by the angle $\theta \in [0, 2\pi] = \mathbb{D}$,

$$x(\theta, t) = X_f(t) + R(t) \begin{pmatrix} \cos \theta \\ \sin \theta \end{pmatrix}$$

Here, the time dependence of $X_f(t)$ and $R(t)$ reflect the temporal evolution of the time-dependent setup of the pendulum. The temporal evolution of the pendulum will be described in terms of the generalized coordinate $\theta(t)$.

Let \mathbf{q} be the generalized coordinates of a system and $\mathbf{x}(\mathbf{q})$ the associated configuration vector of the system. It will be provided in Cartesian coordinates from the point of view of an observer who is at rest. Hence, \mathbf{x} is a vector with all properties discussed in Chapter 2. In contrast, \mathbf{q} will in general only be a tuple of functions that provide a convenient parameterization of valid configurations. We address the situation where the forces in the system are conservative, arising from a potential energy $\Phi(\mathbf{x}(\mathbf{q}), t)$. Moreover, we assume that the potential energy can be represented as a sum of $\Phi_c(\mathbf{x}(\mathbf{q}), t)$ and $U(\mathbf{x}(\mathbf{q}), t)$. The contribution $\Phi_c(\mathbf{x}(\mathbf{q}), t)$ accounts for forces that constraint the coordinates of the system such that they comply with positions $\mathbf{x}(\mathbf{q})$. The part $U(\mathbf{x}(\mathbf{q}), t)$ accounts for all other forces.

We will now explore the implications of the principle of least action for variations of the path that refer only to accessible coordinates. For the k th coordinate of the variation we write

$$\delta x_k = x_k(\mathbf{q} + \delta \mathbf{q}, t) - x_k(\mathbf{q}, t) = \sum_{v=1}^d \frac{\partial x_k}{\partial q_v} \delta q_v$$

and for the associated time derivative we have

$$\delta \dot{x}_k = \frac{d}{dt} \delta x_k = \sum_{v=1}^d \frac{\partial \dot{x}_k}{\partial q_v} \delta q_v + \sum_{v=1}^d \frac{\partial x_k}{\partial q_v} \delta \dot{q}_v$$

As a consequence the variation of the Lagrangian takes the form

$$\delta \mathcal{L} = \delta \mathbf{x} \cdot \nabla_{\mathbf{x}} \mathcal{L} + \delta \dot{\mathbf{x}} \cdot \nabla_{\dot{\mathbf{x}}} \mathcal{L} = \delta \mathbf{x} \cdot (\mathbf{F}_c + \mathbf{F}_e) + \delta \dot{\mathbf{x}} \cdot m \dot{\mathbf{x}}$$

where \mathbf{F}_c represent the constraint forces. We consider variations $\delta \mathbf{x}$ that relate trajectories complying with the constraints such that $\delta \mathbf{x} \cdot \mathbf{F}_c = 0$. Therefore, in the setting of generalized coordinates one need not account for constraint forces.⁴ We will now express the variation of the Lagrangian in terms of the variations of the generalized coordinates,

$$\begin{aligned} \delta \mathcal{L} &= \sum_{k=1}^D \left[\delta x_k \frac{\partial \mathcal{L}}{\partial x_k} + \delta \dot{x}_k \frac{\partial \mathcal{L}}{\partial \dot{x}_k} \right] \\ &= \sum_{k=1}^D \left[\left(\sum_{v=1}^d \frac{\partial x_k}{\partial q_v} \delta q_v \right) \frac{\partial \mathcal{L}}{\partial x_k} + \sum_{v=1}^d \left(\frac{\partial \dot{x}_k}{\partial q_v} \delta q_v + \frac{\partial x_k}{\partial q_v} \delta \dot{q}_v \right) \frac{\partial \mathcal{L}}{\partial \dot{x}_k} \right] \\ &= \sum_{v=1}^d \delta q_v \sum_{k=1}^D \left(\frac{\partial x_k}{\partial q_v} \frac{\partial \mathcal{L}}{\partial x_k} + \frac{\partial \dot{x}_k}{\partial q_v} \frac{\partial \mathcal{L}}{\partial \dot{x}_k} \right) + \sum_{v=1}^d \delta \dot{q}_v \sum_{k=1}^D \frac{\partial x_k}{\partial q_v} \frac{\partial \mathcal{L}}{\partial \dot{x}_k} \end{aligned}$$

⁴ This constraint is commonly denoted as *d'Alembert's principle*.

On the other hand

$$\begin{aligned}\frac{\partial \mathcal{L}(x(\mathbf{q}, t), \dot{x}(\mathbf{q}, \dot{\mathbf{q}}, t), t)}{\partial q_v} &= \sum_{k=1}^D \left(\frac{\partial x_k}{\partial q_v} \frac{\partial \mathcal{L}}{\partial x_k} + \frac{\partial \dot{x}_k}{\partial q_v} \frac{\partial \mathcal{L}}{\partial \dot{x}_k} \right) \\ \frac{\partial \mathcal{L}(x(\mathbf{q}, t), \dot{x}(\mathbf{q}, \dot{\mathbf{q}}, t), t)}{\partial \dot{q}_v} &= \sum_{k=1}^D \frac{\partial \mathcal{L}(x(\mathbf{q}, t), \dot{x}(\mathbf{q}, \dot{\mathbf{q}}, t), t)}{\partial \dot{x}_k} \frac{\partial \dot{x}_k}{\partial \dot{q}_v} \\ &= \sum_{k=1}^D \frac{\partial \mathcal{L}}{\partial \dot{x}_k} \frac{\partial}{\partial \dot{q}_v} \left(\frac{\partial x_k}{\partial t} + \sum_{\mu=1}^d \frac{\partial x_k}{\partial q_\mu} \dot{q}_\mu \right) \\ &= \sum_{k=1}^D \frac{\partial \mathcal{L}}{\partial \dot{x}_k} \frac{\partial x_k}{\partial q_v}\end{aligned}$$

Therefore,

$$\begin{aligned}\delta S &= \int dt \delta \mathcal{L} = \int dt \sum_{v=1}^d \left(\delta q_v \frac{\partial \mathcal{L}}{\partial q_v} + \delta \dot{q}_v \frac{\partial \mathcal{L}}{\partial \dot{q}_v} \right) \\ &= \int dt \sum_{v=1}^d \delta q_v \left(\frac{\partial \mathcal{L}}{\partial q_v} - \frac{d}{dt} \frac{\partial \mathcal{L}}{\partial \dot{q}_v} \right)\end{aligned}$$

The equations of motion are derived from the Lagrangian, Definition 6.5, by Algorithm 6.1.

Definition 6.5: Lagrangian in generalized coordinates

The Lagrange function \mathcal{L} amounts to the difference of the kinetic energy T and the potential energy U of the system,

$$\mathcal{L} = T - U = \sum_{\alpha} \frac{m_{\alpha}}{2} \dot{x}_{\alpha}^2(\mathbf{q}) - U(\mathbf{x}(\mathbf{q})) \quad (6.2.5)$$

Constraint forces are not considered.

Algorithm 6.1: Euler Lagrange EOMs

- Identify generalized coordinates \mathbf{q} that describe the admissible configurations of the system.
- Determine $\mathbf{x}(\mathbf{q})$, and the resulting expression of the potential energy in terms of \mathbf{q} ,

$$U(\mathbf{q}) = U(\mathbf{x}(\mathbf{q}))$$

- Evaluate the kinetic energy based on the chain rule

$$T(\mathbf{q}, \dot{\mathbf{q}}) = \sum_{\alpha} \frac{m_{\alpha}}{2} \dot{x}_{\alpha}^2(\mathbf{q}) = \sum_{\alpha} \frac{m_{\alpha}}{2} \left(\sum_i \frac{\partial x_{\alpha}}{\partial q_i} \dot{q}_i \right)^2$$

where x_{α} is the α -component of the configuration vector \mathbf{x} and m_{α} the mass of the associated particle.

Hence, we establish the Lagrange function

$$\mathcal{L}(\mathbf{q}, \dot{\mathbf{q}}) = T(\mathbf{q}, \dot{\mathbf{q}}) - U(\mathbf{q})$$

expressed in terms of the generalized coordinates \mathbf{q} and their time derivatives $\dot{\mathbf{q}}$.

d) Determine the EOM for the component q_i of q by evaluating the *Euler-Lagrange equation*

$$\frac{d}{dt} \frac{\partial \mathcal{L}}{\partial \dot{q}_i} = \frac{\partial \mathcal{L}}{\partial q_i} \quad (6.2.6)$$

In the next section we will apply the formalism to models with a single degree of freedom.

6.2.4 Self Test

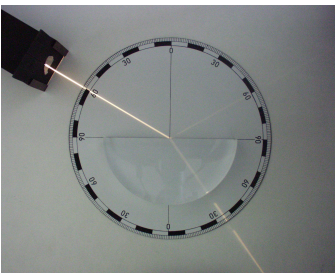
Problem 6.3. Shortest path on a catenoid

In footnote 3 we pointed out that it is a good idea to parameterize the paths on a body of revolution in terms of $z(\theta)$ rather than $\theta(z)$.

Adopt the latter parameterization and work out for yourself that this leads to a second order ODE while the former one provides a conserved quantity, and subsequently immediately a first order ODE.

Problem 6.4. Fermat's principle

Fermat's principle states that a light beam propagates along a path minimizing the flight time. When passing from air into glass it changes direction according to Snellius' refraction law. Here, we consider a setting where the beam starts in air at the position, $(x, y) = (0, 0)$, to the top left in the figure, with coordinates where \hat{x} points downwards and \hat{y} to the right. The path of the light is described by a function $y(x)$. We require that beam passes from air into the glass at the position (a, u) such that it will eventually proceed through the prescribed position (b, w) in the glass. The speed of light in air and in glass will be denoted as c_A and c_G , respectively.



© Zátónyi Sándor (ifj.) Fizped (talk)
CC BY-SA 3.0, wikimedia commons

a) Show that the time of flight T for a (hypothetical) trajectory $y(x)$ with derivative $y'(x)$ can be determined as follows

$$T = c_A^{-1} \int_0^a dx \sqrt{1 + (y'(x))^2} + c_G^{-1} \int_a^b dx \sqrt{1 + (y'(x))^2}.$$

b) In the following we consider a glass body with a planar surface, and align the coordinates such that glass surface is aligned parallel to the y -axis. Hence, we know that the light passes from air to glass at the fixed position a , but we still have to determine u . Determine δT for a variation $y(x) + \delta y(x)$ of the trajectory. What does this imply for $\delta y(x)|_{x=0}$, $\delta y(x)|_{x=a}$ and $\delta y(x)|_{x=b}$? What does it imply for the boundary terms that arise from the integration by parts, when determining δT ?

c) Show that the beam must go in a straight line in air and in glass. Show that this implies that

$$T(u) = \frac{1}{c_A} \sqrt{u^2 + a^2} + \frac{1}{c_G} \sqrt{(w - u)^2 + (b - a)^2}.$$

Derive Snellius' law from the condition that $0 = dT(u)/du$.

- d) Snellius' Law can also be directly obtained from Fermat's principle. How?

Problem 6.5. Stability of soap films

When a soap film is suspended between two rings, it takes a cylinder-symmetric shape of minimal surface area. We discuss here the form of the film for rings of radius R_0 and R_1 positioned at the height x_0 and x_1 , respectively. At the Mathematikum in Gießen there is a nice demonstration experiment: x_0 is the surface height of soap solution in a vessel around the platform where the children are standing, and x_1 is the height of the ring pulled upwards by the children.

- a) Let $w(x)$ be the radius of the cylinder-symmetric soap films at the vertical position x . Sketch the setup and mark the relevant notations for the problem.
- b) Show that the surface area A of the soap film takes the form

$$A = \int_{x_0}^{x_1} dx w(x) f(w'(x)),$$

Here, the factor $f(w'(x))$ takes into account that the area is larger when the derivative $w'(x) = dx/dx$ increases. Determine the function $f(w'(x))$ in this expression.

- c) Show that A is extremal for shapes $w(x)$ that obey the differential equation

$$w''(x) = \frac{1 + (w'(x))^2}{w(x)}.$$

- d) Determine the solutions of the differential equation.

Hint: Rewrite the equation into the form

$$\frac{w'(x) w''(x)}{1 + (w'(x))^2} = \frac{w'(x)}{w(x)}.$$

- e) Consider now solutions with $-x_0 = x_1 = a$ and $R_0 = R_1 = R$, and denote the radius at the thinnest point of the soap film as w_0 . Show that w_0 is the solution of

$$\frac{R}{a} = \frac{w_0}{a} \cosh \frac{a}{w_0}.$$

- f) Sketch R/a as function of a/w_0 . For given R and a you can then find w_0 . For small separation of the rings you should find two solutions. What happens when one slowly rises the ring? Will an adult ever manage to pull up the ring to head height before the film ruptures?



© Mathematikum Gießen
<http://mathematikum.df-kunde.de/Wanderausstellung/index.php?m=2&la=de&id=314>

6.3 Dynamics with one degree of freedom

We will now illustrate the application of the Lagrange formalism for three examples with a single degree of freedom of the motion:

1. The mathematical pendulum, Example 6.1, will give a first idea of how to find EOMs with the Lagrange formalism. This EOM can also easily be found by other approaches. It serves here to illustrate problems where one adopt 2D polar coordinates.

2. The motion of a pearl on a rotating ring constitutes a system with an explicit time dependence. In that case the Lagrange formalism dramatically simplifies the the derivation of the EOM. We will also discuss for this model how to account for dissipative forces and we will see how the solutions of a problem can change qualitatively upon varying a parameter. In this example we will adopt spherical coordinates.

3. The motion of a weight on a carousel we will discussed as an example of a system that needs a dedicated treatment for the description of admissible positions. The discussion will be based on cylindrical coordinates.

6.3.1 The EOM for the mathematical pendulum

The parameterization introduced in Example 6.1 provides the kinetic energy

$$T = \frac{M}{2} \dot{x}^2 = \frac{M}{2} L^2 \dot{\theta}^2 \hat{\theta}(\theta(t))^2 = \frac{M}{2} L^2 \dot{\theta}^2$$

and the potential energy in the gravitational field

$$U = -Mg \cdot x = -ML \hat{R}(\theta(t)) \cdot g = -MLg \cos \theta(t)$$

since $g = g \hat{R}(0)$.

Consequently,

$$\mathcal{L} = \frac{M}{2} L^2 \dot{\theta}^2 + MgL \cos \theta(t)$$

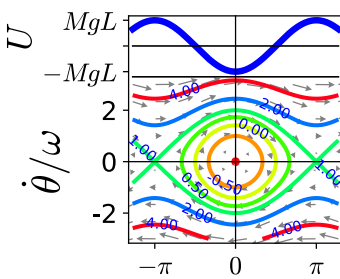
$$\Rightarrow ML^2 \ddot{\theta}(t) = \frac{d}{dt} \frac{\partial \mathcal{L}}{\partial \dot{\theta}} = \frac{\partial \mathcal{L}}{\partial \theta} = -MgL \sin \theta(t)$$

$$\Rightarrow \ddot{\theta}(t) = -\frac{g}{L} \sin \theta(t) \tag{6.3.1}$$

The EOM (6.3.1) can be integrated once by multiplication with $2\dot{\theta}(t)$

$$\begin{aligned} \dot{\theta}^2(t) - \dot{\theta}^2(t_0) &= \int_{t_0}^t dt 2\dot{\theta}\ddot{\theta} = \int_{t_0}^t dt 2\dot{\theta} \left(-\frac{g}{L} \sin \theta(t)\right) \\ &= 2 \int_{\theta(t_0)}^{\theta(t)} d\theta \frac{d}{d\theta} \left(\frac{g}{L} \cos \theta\right) = 2 \frac{g}{L} (\cos \theta(t) - \cos \theta(t_0)) \end{aligned}$$

This is a Mattheui differential equation. For most initial conditions it can not be solved by simple means. However, the first integral provides the phase-space trajectories $\dot{\theta}(\theta)$ for every given set of initial conditions $(\theta(t_0), \dot{\theta}(t_0))$,



$$\dot{\theta} = \pm \sqrt{\dot{\theta}^2(t_0) + \frac{2g}{L} (\cos \theta(t) - \cos \theta(t_0))}$$

The phase-space portrait is shown in Figure 6.5. There are trivial solutions where the pendulum is resting without motion at its stable and unstable rest positions $\theta = 0$ and $\theta = \pi$. These positions are denoted as *fixed points* of the dynamics. There are closed circular trajectories close to the minimum, $\theta = 0$, of the potential where it is harmonic to a good approximation. These are solutions with energies $0 < 1 + E/MgL \lesssim 1$.

For larger amplitudes the amplitude of the swinging grows, and the circular trajectories get deformed. When E approaches MgL the phase-space trajectories arrive close to the tipping points $\theta = \pm\pi$ where they form very sharp edges. For θ close to $\theta = \pm\pi$ the trajectories look like the hyperbolic scattering trajectories for the potential $-ax^2/2$ that was discussed in Problem 4.25. When the non-dimensional energy is exactly one, the pendulum starts on top, goes through the minimum and returns to the top again. Apart from the fixed points, this is the only case where the evolution can be obtained in terms of elementary functions. For the initial condition $\dot{\theta}(t_i) = 0$ and $\cos \theta_i = -1$ we find

$$\omega^{-1} \dot{\theta}_H(t) = \pm \sqrt{2 + 2 \cos \theta_H(t)} = \pm 2 \cos \frac{\theta_H(t)}{2}$$

The same equation is also obtained for the initial condition $\theta_0 = 0$ and $\dot{\theta}(t_0) = \sqrt{2g/L}$ half-way on the way from the top back to the top. For this initial condition the ODE for $\dot{\theta}_H$ can be integrated, and we find

$$\begin{aligned} \pm 2\omega(t-t_0) &= \int_0^{\theta(t)} \frac{d\theta}{\cos \frac{\theta}{2}} = \ln \tan \frac{\theta + \pi}{4} \\ \Rightarrow \theta_H(t) &= -\pi + 4 \arctan e^{\pm 2\omega(t-t_0)} \end{aligned} \quad (6.3.2)$$

The \pm signs account for the possibility that the pendulum can move clockwise and counterclockwise. The counterclockwise trajectory is shown in Figure 6.6. In the limit $t \rightarrow -\infty$ it starts in the unstable fixed point $\theta = -\pi$. It falls down till it reaches the minimum $\theta = 0$ at time t_0 , and then it rises again, reaching the maximum $\theta = \pi$ for time $t \rightarrow \infty$. Such a trajectory is called a homocline.

Definition 6.6: Homoclines and Heteroclines

Homoclines and *heteroclines* are trajectories that approach a fixed point of a dynamics in their infinite past and future. A homocline returns to the same fixed point from where it started. A heterocline connects two different fixed points.

The take-home message of this example is that the minima and maxima of a potential organize the phase space flow. Close to each minimum a conservative system will have closed trajectories that

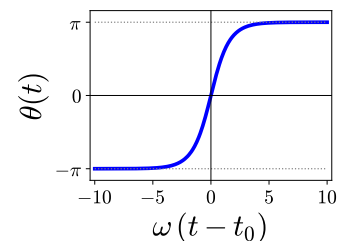


Figure 6.6: Anticlockwise moving heterocline for the mathematical pendulum.

represent oscillations in a potential well. The well is confined by maxima to the left and right of the minimum of the potential. When these maxima have different height there is a homoclinic orbit coming down from and returning to the shallower maximum. When they have the same height, they are connected by heteroclinic orbits. Thus, the homoclines and heteroclines divide the phase space into different domains. Initial conditions within the same domain show qualitatively the same dynamics. Initial conditions in different domains feature qualitatively different dynamics. For the mathematical pendulum the heteroclines divide phase space into three domains, up to the 2π translation symmetry of θ :

- There are trajectories oscillating around $\theta = 0$, with energies smaller than MgL . The region of these oscillations is bounded by the heteroclines provided in Equation (6.3.2).
- Trajectories with initial conditions lying above the anticlockwise moving heterocline will persistently rotate anticlockwise and never reverse their motion.
- Trajectories with initial conditions lying below the clockwise moving heterocline will persistently rotate clockwise and never reverse their motion.

The general strategy for sketching phase-space plots is summarized in the following algorithm and illustrated in Figure 6.7.

Algorithm 6.2: Phase space plots

- Identify the minima and maxima of the potential. Mark the minima as (marginally) stable fixed points with velocity zero. Mark the maxima as unstable fixed points with velocity zero.
- Identify the fate of trajectories departing from the unstable fixed points. Identify to this end the closest positions on the potential that have the same height as the maximum. When it is another extremum the orbit will form an heterocline. Otherwise, it will be reflected and return to the initial maximum, forming a homocline. If there is no further point of the same height, the trajectory will escape to infinity.
- Add characteristic trajectories close to the minima, in between and outside of homo- and heteroclines.

In these steps it is advisable to

- Observe the symmetries of the system. To the very least the plot is symmetric with respect to reflection at the horizontal axis, i. e. swapping the sign of the velocity.
- Observe energy conservation (if it applies): The modulus of the velocity takes a local minimum for a maximum of

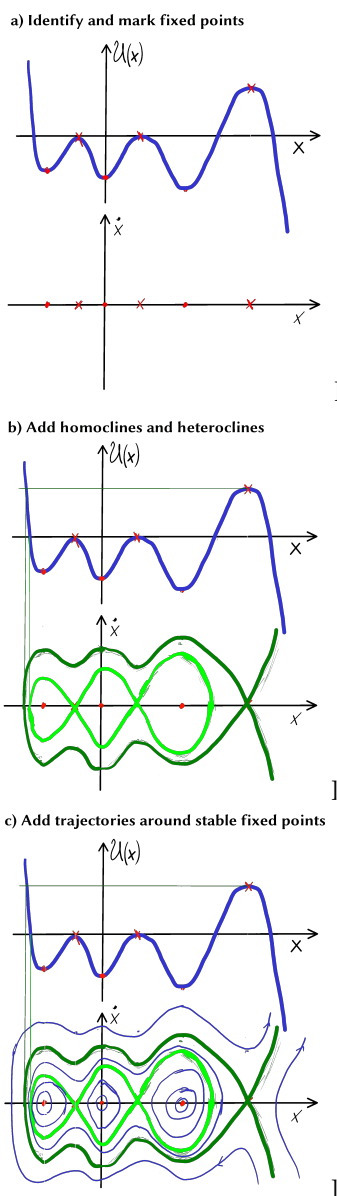


Figure 6.7: Step by step sketch of a phase-space plot.

the potential, and a local maximum for a minimum of the potential.

6.3.2 The EOM for a pearl on a rotating ring

We consider a pearl of mass M that can freely move on a ring. The ring is mounted vertically in the gravitational field and it spins with angular velocity Ω around its vertical symmetry axis. The setup constrains the position of the pearl to lie on a spherical shell. The position of the pearl on the ring is fully described by the angle $\theta(t)$ of the deflection of the pearl from the direction of gravity (see Figure 6.8). In addition we must specify the orientation of the ring. This will be done by the angle $\phi(t) = \Omega t$ that enters as a parameter in this time-dependent problem. Hence, the position of the pearl is most conveniently specified in terms of polar coordinates (R, θ, ϕ) where R takes the constant value ℓ , and $\phi(t) = \Omega t$ enters as a time-dependent parameter.

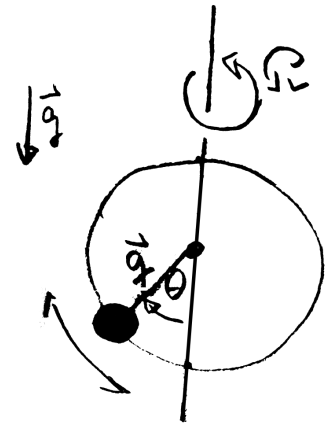


Figure 6.8: Motion of a pearl moving on a ring rotating with a fixed frequency Ω .

Theorem 6.3: Basis vectors for spherical coordinates

Let $\{\hat{x}, \hat{y}, \hat{z}\}$ be a fixed Cartesian basis of \mathbb{R}^3 , and (R, θ, ϕ) be the spherical coordinates associated to a point $(x, y, z) \in \mathbb{R}^3$. Then

- $R = \sqrt{x^2 + y^2 + z^2}$ is the distance from the origin
- $\theta = \arctan(\sqrt{x^2 + y^2}/z)$ is the angle with respect to \hat{z} ,
- $\phi = \arctan(y/x)$ the angle with respect to \hat{x} of the projection of the position into the (x, y) plane.

We denote the vector from the origin to (R, θ, ϕ) as $R \hat{R}(\theta, \phi)$. Then the following statements apply

- a) $\hat{\theta} = \partial_\theta \hat{R}$ is a vector pointing along the grant circle of the unit sphere selected by (θ, ϕ) and \hat{z}
- b) $\hat{\phi} = \hat{R} \times \hat{\theta}$ is a vector tangential to the unit sphere at (θ, ϕ) and vertical to \hat{z}
- c) For every $\theta \in [0, \pi]$ and $\phi \in [0, 2\pi)$ the vectors $\{\hat{R}, \hat{\theta}, \hat{\phi}\}$ form a right-handed orthonormal basis of \mathbb{R}^3 .

add sketch of unit vectors for spherical coordinates

Remark 6.5. The directions of the basis vectors $\{\hat{R}, \hat{\theta}, \hat{\phi}\}$ depend on θ and ϕ . ◻

Theorem 6.4: Derivatives of the basis vectors for spherical coordinates

The partial θ and ϕ derivatives of the basis vectors $\{\hat{R}, \hat{\theta}, \hat{\phi}\}$ obey the following relations

$$\begin{aligned} \partial_\theta \hat{R} &= \hat{\theta} & \partial_\phi \hat{R} &= \sin \theta \hat{\phi} \\ \partial_\theta \hat{\theta} &= -\hat{R} & \partial_\phi \hat{\theta} &= \cos \theta \hat{\phi} \\ \partial_\theta \hat{\phi} &= 0 & \partial_\phi \hat{\phi} &= -\sin \theta \hat{R} - \cos \theta \hat{\theta} \end{aligned} \quad (6.3.3)$$

Proof. The proofs of Theorems 6.3 and 6.4 are given as Problem 6.6. \square

In polar coordinates the position of the pearl is

$$x(t) = \ell \hat{R}(\theta(t), \phi(t))$$

We adopt the Lagrange formalism to determine the equation of motion for $\theta(t)$, which is the only coordinate in this setting. (The motion of the pearl has a single degree of freedom.)

The potential energy takes the same form as for the pendulum,

$$U = -M g \cdot x = -M g \ell \cos \theta(t).$$

The kinetic energy is obtained based on its velocity

$$\begin{aligned} \dot{x} &= \ell \frac{d}{dt} \hat{R}(\theta(t), \Omega t) = \ell \dot{\theta} \partial_\theta \hat{R}(\theta(t), \Omega t) + \ell \Omega \partial_\phi \hat{R}(\theta(t), \Omega t) \\ &= \ell \dot{\theta} \hat{\theta}(\theta(t), \Omega t) + \ell \Omega \sin \theta(t) \hat{\phi}(\theta(t), \Omega t) \end{aligned}$$

which provides the Lagrange function

$$\mathcal{L}(\theta, \dot{\theta}) = \frac{M}{2} \ell^2 \dot{\theta}^2 + \frac{M}{2} \ell^2 \Omega^2 \sin^2 \theta(t) + M g \ell \cos \theta(t)$$

It only differs from the expression for the spherical pendulum by the fact that $\phi(t)$ is not a coordinate whose evolution must be determined from an EOM. Rather it is a parameter $\phi(t) = \Omega t$ provided by the setting of the problem.

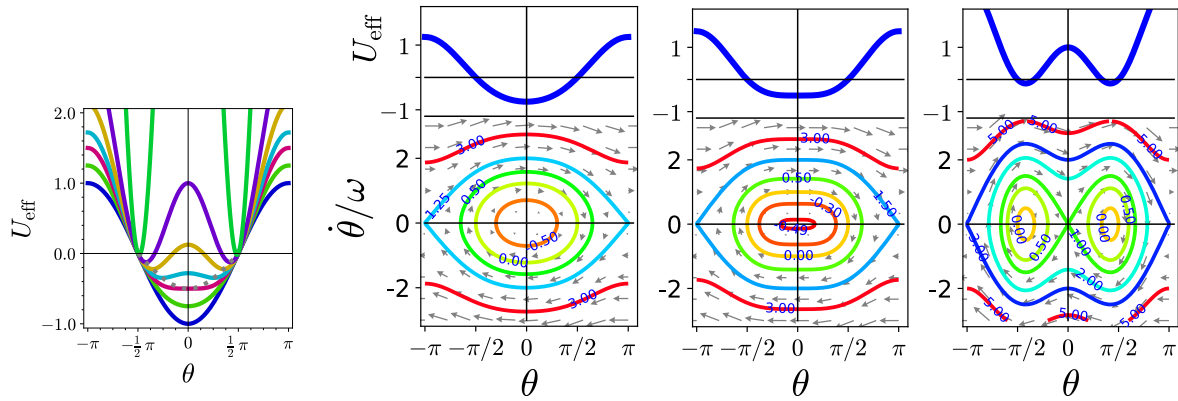
The motion only has a single DOF, $\theta(t)$, with EOM

$$\ddot{\theta}(t) = -\frac{g}{\ell} \sin \theta(t) \left(1 - \frac{\ell \Omega^2}{g} \cos \theta(t) \right) \quad (6.3.4)$$

This EOM can once be integrated by the same strategy adopted for the swing and the spherical pendulum. Thus, one finds the effective potential

$$U_{\text{eff}}(\theta) = -\omega^2 \cos \theta \left[1 - \left(\frac{\Omega}{\omega} \right)^2 \cos \theta \right]$$

Figure 6.9 shows the effective potential and phase space portraits for different values of angular momentum, i. e. of the dimensionless control parameter $\kappa = \Omega/\omega$. For $\kappa < 1$ the phase space has the



same structure as that of a mathematical pendulum, with a stable fixed point at $\theta = 0$. When κ passes through one, this minimum of U_{eff} turns into a maximum, and two new minima emerge at the positions

$$\theta_c = \pm \arccos \kappa^{-2} = \pm \arccos \left(\frac{\omega}{\Omega} \right)^2 \quad (6.3.5)$$

that are indicated by a dotted gray line in the left panel of Figure 6.9. The new maximum at zero is always shallower than the maxima at $\pm\pi$. Hence, it gives rise to two homoclinic orbit that wind around the new stable fixed points. The maxima at $\pm\pi$ will further we connected by heteroclinic orbits. Hence, phase space is divided into five distinct regions. For energies smaller than $U_{\text{eff}}(\theta = 0)$ the trajectories wiggle around one of the stable fixed points. They stay on one side of the ring and oscillate around the angle θ_c . There are two regions of this type because the pearl can stay on both sides of the ring. For $U_{\text{eff}}(\theta = 0) < E < U_{\text{eff}}(\theta = \pi)$ the trajectories show oscillations back and forth between the two sides of the ring, For $E > U_{\text{eff}}(\theta = \pi)$ they rotate around the ring in clockwise or counter-clockwise direction for $\dot{\theta} < 0$ or $\dot{\theta} > 0$, respectively.

There are two take-home message from this example:

1. There are no conservation laws in the dynamics when there are explicitly time-dependent constraints. Hence, the strategies of Chapter 4 to establish and discuss the EOM can no longer be applied. However, the Lagrange formalism still provides the EOM in a straightforward manner.

2. In general, the structure of the phase-space flow changes upon varying the dimensionless control parameters of the dynamics. These changes are called bifurcations, and they are a very active field of contemporary research in theoretical mechanics. The pearl on the ring features a pitchfork bifurcation since the positions of the fixed points resemble the shape of a pitch fork (see Figure 6.10).

Figure 6.9: The left panel shows the effective potential for the pearl on a ring for parameter values $(\Omega/\omega) \in \{0, 2^{-1/2}, 1, 1.2, 1.5, 2, 5\}$ from bottom to top. The subsequent panels show phase-space portraits of the motion for $\Omega/\omega = 2^{-1/2}, 1$, and 2 , respectively.

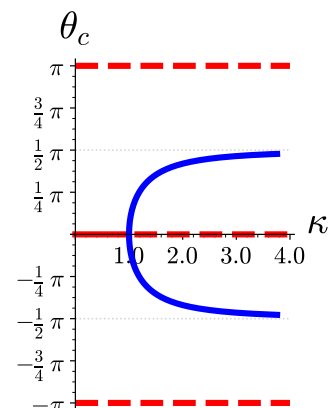


Figure 6.10: Parameter dependence of the positions of the fixed points of the rotation governor. Solid lines mark stable fixed points, and unstable fixed

Definition 6.7: Pitchfork bifurcation

Upon variation of a parameter p a stable fixed point x_* of a one-dimensional ODE may lose stability at some parameter p_c , turning into an unstable fixed point. In that case one will encounter one of the following scenarios:

supercritical pitchfork bifurcation At p_c two new stable fixed points emerge to its left and right of x_* .

subcritical pitchfork bifurcation There were unstable fixed points to the left and right of x_* that merge with x_* at the parameter p_c . Subsequently there is only a single unstable fixed point.

Remark 6.6. The supercritical pitchfork bifurcation is commonly simply denoted as pitchfork bifurcation. □

Remark 6.7. In classical mechanics a pitchfork bifurcation, Figure 6.10, emerges whenever a minimum of a potential is deformed to turn it into a maximum that is then surrounded by two minima on both sides, as shown in Figure 6.9.

The supercritical pitchfork bifurcation refers to a situation where we initially have a minimum surrounded by two maxima, and then the minimum is pushed until it disappears. When this happens the maxima approach each other, and eliminate the dent in between. An example is provided in Problem 6.8. □

add fig for supercritical pitchfork

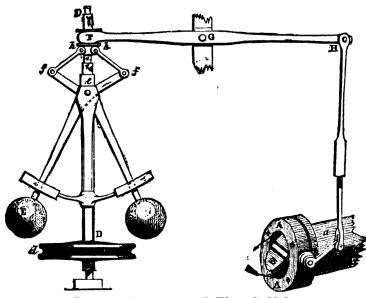


FIG. 4.--Governor and Throttle-Valve.

Figure 6.11: Rotational governor and throttle valve. When the rotation speed exceeds a critical value the weights move outward and the arm opens a valve that reduces pressure in the steam engine. (Image from “Discoveries & Inventions of the Nineteenth Century” by R. Routledge, 13th edition, published 1900, Public domain, via Wikimedia Commons)

6.3.3 Centrifugal Governor

The sharp increase of θ_c in Equation (6.3.5), when the rotation frequency ω rises beyond Ω is used in a feedback mechanism of the governor to control the rotation speed of steam engines (Figure 6.11).

Oscillations around the stable fixed points is an undesirable feature of the governor such that some dissipation is welcome. We revisit Equation (6.2.1) to extend the Lagrange formalism for forces that do not derive from a potential

$$\begin{aligned} 0 &= - \int_{t_1}^{t_F} dt \frac{d}{dt} (\delta x \cdot m \dot{x}) = - \int_{t_1}^{t_F} dt (\delta \dot{x} \cdot m \dot{x} + \delta x \cdot m \ddot{x}) \\ &= - \int_{t_1}^{t_F} dt (\delta \dot{x} \cdot \nabla_x \mathcal{L} + \delta x \cdot m (F_d - \nabla_x \Phi)) \\ &= \int_{t_1}^{t_F} dt \delta x \left(-F_d + \nabla_x \mathcal{L} - \frac{d}{dt} \nabla_x \mathcal{L} \right) \end{aligned}$$

Thus, and additional dissipative force $F_d = -\gamma \dot{\theta} \hat{\theta}$ will give rise to an additional additive term in Equation (6.3.4) such that the rotational governor has an EOM

$$\ddot{\theta}(t) = -\frac{g}{\ell} \sin \theta(t) \left(1 - \frac{\ell \Omega^2}{g} \cos \theta(t) \right) - \frac{\gamma}{M} \dot{\theta}(t)$$

and the energy evolves as

$$\frac{d}{dt} \left(\frac{\dot{\theta}^2}{2} + U_{\text{eff}}(\theta) \right) = -\frac{\gamma}{M} \dot{\theta}^2(t)$$

Small friction deflects the trajectories towards smaller values of the effective potential, until the system comes to rest in a stable fixed point. For $\Omega/\omega = 2$ the impact of dissipation $\gamma/M = 0.2$ and 2.0 is shown in Figure 6.12.

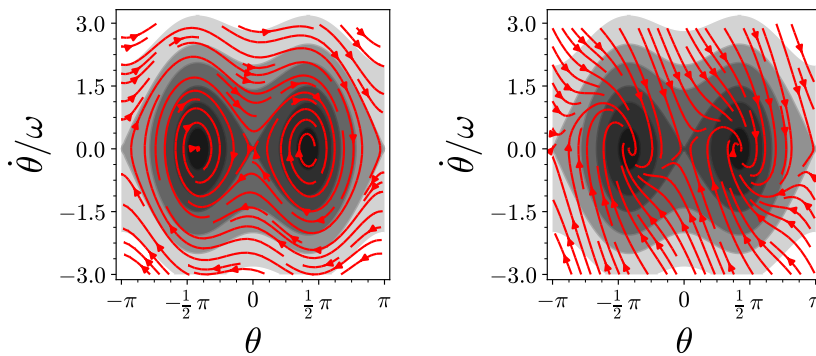


Figure 6.12: Phase-space plot for a rotational governor with rotation frequency $\Omega = 2\omega$. The colors of gray in the background show contour levels of the energy. The streamlines indicated the evolution of the dynamics for (left) weak dissipation, $\gamma = 0.2$, and (right) strong dissipation, $\gamma = 2$, dissipation. Due to dissipation the trajectories acquire a component downwards in energy.

6.3.4 Carousel

The positions in the systems that we treated so far were described in terms of polar coordinates (mathematical pendulum, Section 6.3.1) and spherical coordinates (pearl on a rotating ring, Section 6.3.2). We will now address a system where we adopt *cylindrical coordinates* to describe particle positions: the motion of the beats of a toy carousel that is shown in Figure 6.13. The carousel is composed of four cantilever beams of length R that extend outwards from a vertical axis that is rotating with angular velocity Ω . At the far end of each beam there is a pendulum attached that freely swings in outward direction. The inclination of the pendulum arm towards gravity will be denoted as θ . (Oscillations parallel to the motion of the beams are not be considered.) The pendulum arm has a length L and it carries a weight m . Due to a magnetic contact the pendulum experiences minimal friction in its motion. Henceforth we the focus on the motion of one of the beats.

We pick the origin of the coordinate system on the rotation axes right on the height of the cantilever. The rotation is around the vertical axes characterized the the unit vector \hat{z} . Looking from the top (right panel of Figure 6.13) the pendulum arm sticks out in direction $\phi = \Omega t$. We adopt polar coordinates, as introduced in Remark 6.3, in the horizontal plane vertical to \hat{z} . We denote the position of the fulcrum of the pendulum as $\mathbf{R} = R \hat{r}(\phi)$, and express the vector from the fulcrum to the weight as $L \sin \theta \hat{r}(\phi) - L \cos \theta \hat{z}$.

add sketch of unit vectors for cylindrical coordinates

This amounts to a representation of the position of the mass in terms of *cylindrical coordinates* (see ??).

Theorem 6.5: Basis vectors for cylindrical coordinates

Let $\{\hat{x}, \hat{y}, \hat{z}\}$ be a basis of \mathbb{R}^3 , and $(R = \sqrt{x^2 + y^2}, \phi = \tan(y/x), z)$ be the cylindrical coordinates associated to a point with Cartesian coordinates (x, y, z) . Then

- $R = \sqrt{x^2 + y^2}$ is the distance of the point from the \hat{z} axis
- $\phi = \arctan(y/x)$ the angle with respect to \hat{x} of the projection of the position into the (x, y) plane.

We denote the vector from the origin to (R, ϕ, z) as $\mathbf{x} = z \hat{z} + R \hat{\mathbf{R}}(\phi)$. Then, the following statements apply

- $\hat{\phi} = \partial_\phi \hat{\mathbf{R}}$ and \hat{z} are the horizontal and vertical unit vectors tangential to the surface of a cylinder with axis pointing along \hat{z}
- For every $\phi \in [0, 2\pi)$ the vectors $\{\hat{\mathbf{R}}(\phi), \hat{\phi}(\phi), \hat{z}\}$ form a right-handed orthonormal basis of \mathbb{R}^3 .

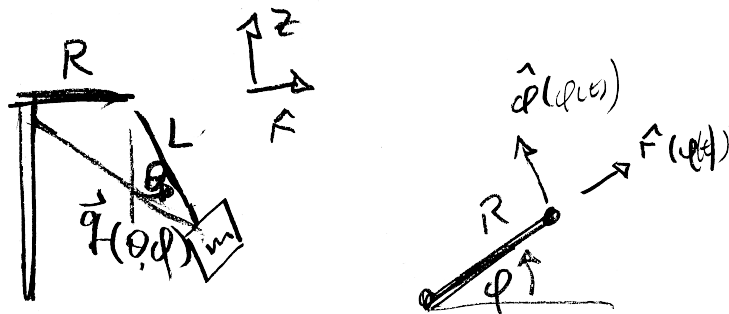
The ϕ -derivatives of $\hat{\mathbf{R}}$ and $\hat{\phi}$ follow the same rules as for polar coordinates, Theorem 6.1.

Proof. The proof is left to the reader. □

The position \mathbf{x} and the velocity $\dot{\mathbf{x}}$ of the weight attached to the carousel are

$$\begin{aligned} \mathbf{x} &= (R + L \sin \theta) \hat{\mathbf{r}}(\Omega t) - L \cos \theta \hat{z} \\ \dot{\mathbf{x}} &= (R + L \sin \theta) \Omega \hat{\phi}(\Omega t) + L \cos \theta \dot{\theta} \hat{\mathbf{r}}(\Omega t) + L \sin \theta \dot{\theta} \hat{z} \end{aligned}$$

Figure 6.13: Experimental setup and description of configurations for a toy carousel.



The kinetic energy and potential energy are

$$T = \frac{m}{2} \dot{x}^2 = \frac{m}{2} \left[L^2 \dot{\theta}^2 + (R + L \sin \theta)^2 \Omega^2 \right]$$

$$V = -mgL \cos \theta$$

and the Euler-Lagrange equation for $\theta(t)$ take the form

$$m L^2 \ddot{\theta}(t) = \frac{d}{dt} \frac{\partial \mathcal{L}}{\partial \dot{\theta}} = \frac{\partial \mathcal{L}}{\partial \theta} = m \Omega^2 (R + L \sin \theta) \cos \theta - mgL \sin \theta$$

We introduce

- the eigenfrequency of the hanging arm, $\omega = \sqrt{g/L}$
- the ratio of frequencies, $\tau = \Omega/\omega$
- the ratio of the length of the arms, $\lambda = R/L$

and absorb ω into the dimensionless time scale. Thus, we find

$$\ddot{\theta} = \tau^2 (\lambda + \sin \theta) \cos \theta - \sin \theta$$

which admits a conserved energy-like quantity

$$\mathcal{E} = \frac{\dot{\theta}^2}{2} + U_{\text{eff}}(\theta)$$

with an effective potential

$$U_{\text{eff}}(\theta) = -\frac{\tau^2}{2} (\lambda + \sin \theta)^2 - \cos \theta \quad (6.3.6)$$

The left panel of Figure 6.14 shows the effective potential for a fixed ratio $L/R = 4$ and different values of Ω/ω . For small frequencies, $\Omega/\omega = 0.2$, the masses are pushed outwards such that the equilibrium position is no longer at $\theta = 0$. Otherwise, the phase space plot looks like the one of a mathematical pendulum. For increasing $\tau = \Omega/\omega$ a shoulder emerges in the potential, and for $\tau > \tau_c \simeq 1.5$ this leads to the emergence of a new minimum with $-\pi/2 < \theta_- < 0$. It is separated from the previous minimum by a maximum at θ_+ with $-\theta_- \gg -\theta_+ > 0$. For $\tau > \tau_c$ there are two stable fixed points that lie in regions surrounded by homoclinic trajectories that start and end at θ_+ . Further outside there are oscillating trajectories that move around both fixed points, and beyond the heteroclinic trajectories that connect the maxima of the potential one finds trajectories that keep rotating in the same direction.

When increasing the rotation frequency beyond τ_c a second stable solution emerges in the system. To find the parameters where it emerges we observe that fixed points emerge at positions θ where the effective force vanishes

$$\begin{aligned} \sin \theta &= \tau^2 (\lambda + \sin \theta) \cos \theta \\ \Rightarrow \lambda_\tau(\theta) &= \frac{\tan \theta}{\tau^2} - \sin \theta \end{aligned}$$

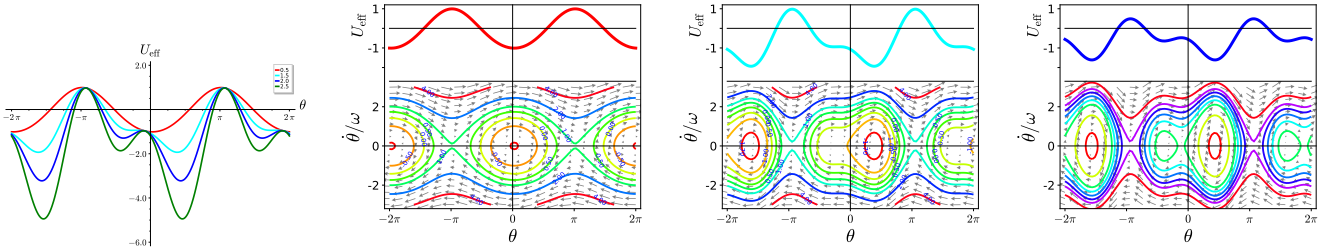


Figure 6.14: The effective potential (left) and phase space plots for the

This equation is solved for a unique angle θ_c when $\lambda_\tau(\theta)$ is monotonic, and potential extrema of $\lambda_\tau(\theta)$ must fulfill

$$0 = \frac{d\lambda}{d\theta} = \frac{1}{\tau^2} \frac{1}{\cos^2 \theta_c} - \cos \theta_c \quad \Rightarrow \quad \cos \theta_c = \tau^{-2/3}$$

Consequently,

for $\tau < 1$ the function $\lambda_\tau(\theta)$ is monotonous such that there is a unique fixed point. It is a minimum.

for $\tau > 1$ the function $\lambda_\tau(\theta)$ has a maximum and a minimum such that there can be up to three fixed point: two minima and a maximum.

The range values $\lambda = R/L$ where there are two minima is bounded by the extrema $\lambda_\tau(\theta_c)$,

$$\begin{aligned} \lambda_c(\theta_c) &= \sin \theta_c \left(\frac{1}{\tau^2 \cos \theta_c} - 1 \right) = \mp \sqrt{1 - \cos^2 \theta_c} \left(\frac{1}{\tau^2 \cos \theta_c} - 1 \right) \\ &= \pm \left(1 - \tau^{-4/3} \right)^{3/2} \end{aligned}$$

Hence, there is a single maximum for $\tau = \Omega/\omega < 1$ and when $R/L > \left(1 - \tau^{-4/3} \right)^{3/2}$ for $\tau > 1$. In Figure 6.15 this conclusion is visualized in a phase diagram where this aspect of the behavior is marked in the parameter plane of the problem, i. e. as function of $\tau = \Omega/\omega$ and $\lambda = R/L$.

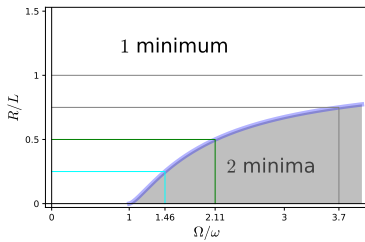


Figure 6.15: Phase diagram with positions of the bifurcations as function of τ and λ .

Definition 6.8: Phase Diagram

A phase diagram for some property of a dynamics is a plot that shows for which parameters this property can be observed.


It is illuminating to observe that the motion of the pearl on the rotating ring is recovered as the special case $R = 0$ of the carousel dynamics. For $\lambda = 0$ the effective potential, Equation (6.3.6), has three critical points for $\tau > 1$, and two of them disappear in a pitchfork bifurcation when they all meet at $\theta = 0$ for $\tau = 1$. In terms of the condition on the forces this happens when at $\theta = 0$ the slope of $\tau^2 \sin \theta$ becomes larger than the one of $\tan \theta$. For $\tau > 0$

there will be three intersections of the two functions rather than a single one.

The scenario for $\lambda > 0$ is different. This is most easily seen by considering a value $\tau > 1$ and increasing λ . For $\lambda = 0$ there are intersections of $\tau^2 \sin \theta$ and $\tan \theta$ at $\theta \in \{0, \pm\theta_c\}$. Increasing λ amounts to a vertical displacement of the sine function. The critical points that are initially at $\pm\theta_c$ will then move right and the one in the middle moves to the left because $\lambda + \sin \theta > 0$ for $\lambda > 0$ and $\theta = 0$. Therefore, the minimum to the right will persist, and the minimum to the left will at some point merge with the maximum and they will annihilate. Such a scenario is called a saddle-node bifurcation.

Definition 6.9: Saddle-node bifurcation

We consider a one-dimensional ODE for a real variable x that depends on a parameter p . In a certain range of parameters $p \in \mathbb{U}$ the system has a stable fixed point at x_s and an unstable fixed point at x_u . A saddle-node bifurcation emerges at $p_* \in \partial\mathbb{U}$ when $x_u(p)$ and $x_s(p)$ meet and annihilate at $x_* = x_u(p_*) = x_s(p_*)$.

Remark 6.8. In classical mechanics a saddle-node bifurcation emerges when the height difference between a minimum and a neighboring maximum of a potential diminishes, becomes zero in a saddle point, and subsequently, the potential will no longer have no critical point in the considered region. 

6.3.5 Self Test

Problem 6.6. Basis vectors for spherical coordinates

- a) Verify by explicit calculation that \hat{R} , $\hat{\theta}$, and $\hat{\phi}$ obey the relations

$$\hat{\theta} = \frac{\partial \hat{R}}{\partial \theta} \quad \text{and} \quad \hat{\phi} = \hat{R} \times \hat{\theta},$$

and that they form an orthonormal basis.

- b) How is $\hat{\phi}$ related to $\partial \hat{R} / \partial \phi$?
- c) Verify also the other expressions, Equation (6.3.3), for the partial derivatives of the basis vectors.

Problem 6.7. Phase-space analysis for a pearl on a rotating ring

- a) Evaluate $\dot{x}(t) = \ell \hat{R}(\theta(t), \Omega t)$ based on the relations established in Problem 6.6.
- b) Determine the kinetic energy T and the potential energy V of the pearl.
- c) Fill in the steps in the derivation of the EOM for θ , as provided in Equation (6.3.4).

- d) Verify that neither the energy nor any of the coordinates of momentum and angular momentum are conserved for this motion.

Problem 6.8. An EOM with a subcritical pitchfork bifurcation

Consider the equation of motion

$$\ddot{x} = x(x^2 - 1)(x^2 - a)$$

where the right-hand side is considered as a dimensionless force on a particle that resides at the dimensionless position $x \in \mathbb{R}$. The dynamics depends on the parameter $a \in \mathbb{R}$.

- a) Determine the fixed points of the dynamics, and verify that $x = 0$ is a stable fixed point for $a < 0$ and an unstable fixed point for $a > 0$.
- b) Verify that the dynamics has a subcritical pitchfork bifurcation at $a = 0$.
- c) Sketch the bifurcation diagram, i.e. a plot analogous to Figure 6.10 where the positions of the fixed points are indicated as function of a . Use solid lines for stable fixed points and dotted lines for unstable fixed points.
- d) Sketch the form of the potential for dynamics with $a < 0$, $0 < a < 1$, and $a > 1$.

Problem 6.9. An EOM with a saddle-node bifurcation

Consider the equation of motion

$$\ddot{x} = (1 - x)(x^2 + a)$$

where the right-hand side is considered as a dimensionless force on a particle that resides at the dimensionless position $x \in \mathbb{R}$. The dynamics depends on the parameter $a \in \mathbb{R}$.

- a) Determine the fixed points of the dynamics, and verify that the EOM has three fixed points for $a < 0$, two fixed points for $a = 1$, and a single fixed point for $a > 0$.
- b) Sketch the bifurcation diagram, i.e. a plot analogous to Figure 6.10 where the positions of the fixed points are indicated as function of a . Use solid lines for stable fixed points and dotted lines for unstable fixed points.
- c) Sketch the form of the potential for dynamics with $a < -1$, $-1 < a < 0$, and $a > 0$.

6.4 Dynamics with two degrees of freedom

In Section 6.3 we discussed the EOM of systems with one degree of freedom. In the present section this analysis will be extended to

systems with two degrees of freedom. Again the discussion will be based on three examples:

1. For the spherical pendulum we will learn how to exploit conservation laws to reduce a two degrees of freedom dynamics based on the solution of a dynamics with a single degree of freedom.
2. The Foucault pendulum will allow us to further explore the impact of rotation.
3. For the double pendulum we will see that conservation laws can in general at best be found for special parameters of the dynamics.

6.4.1 The EOM for the spherical pendulum

The spherical pendulum describes the motion of a mass M that is mounted on a bar of fixed length ℓ whose other end is fixed to a pivot. Thus, the position of the mass is constrained to a spherical shell. We adopt spherical coordinates to describe the position as

$$\mathbf{x}(t) = \ell \begin{pmatrix} \sin \theta(t) \cos \phi(t) \\ \sin \theta(t) \sin \phi(t) \\ -\cos \theta(t) \end{pmatrix} = \ell \hat{\mathbf{R}}(\theta(t), \phi(t))$$

Note that the angle θ is measured here with respect the negative z axis, in contrast to the definition adopted in Theorem 6.3. As a consequence, we have now

$$\hat{\boldsymbol{\theta}}(\theta, \phi) = \begin{pmatrix} \cos \theta \cos \phi \\ \cos \theta \sin \phi \\ \sin \theta \end{pmatrix} \quad \text{and} \quad \hat{\boldsymbol{\phi}}(\theta, \phi) = \begin{pmatrix} -\sin \theta \sin \phi \\ \sin \theta \cos \phi \\ 0 \end{pmatrix}$$

with $0 < \theta < \pi$ and $0 \leq \phi < 2\pi$. The same rules for the derivatives apply as provided in Theorem 6.4, but now $\{\hat{\mathbf{R}}, \hat{\boldsymbol{\phi}}, \hat{\boldsymbol{\theta}}\}$ provides a right handed coordinate system, i. e. $\hat{\mathbf{R}} \times \hat{\boldsymbol{\theta}} = -\hat{\boldsymbol{\phi}}$.

The angle θ denotes the angle between the position the mass and the gravitational field. Consequently, the potential energy in the gravitational field is obtained

$$U = -M \mathbf{g} \cdot \mathbf{x} = -M g \ell \cos \theta(t).$$

The angle ϕ describes in which direction the mass is deflected from the vertical line, in a plane orthogonal to the action of gravity (see Figure 6.16).

For the velocity we find based on the chain rule and the derivatives of the unit vectors, Equation (6.3.3),

$$\begin{aligned} \dot{\mathbf{x}} &= \ell \dot{\theta} \partial_{\theta} \hat{\mathbf{R}}(\theta(t), \phi(t)) + \ell \dot{\phi} \partial_{\phi} \hat{\mathbf{R}}(\theta(t), \phi(t)) \\ &= \ell \dot{\theta} \hat{\boldsymbol{\theta}}(\theta(t), \phi(t)) + \ell \dot{\phi} \sin \theta(t) \hat{\boldsymbol{\phi}}(\theta(t), \phi(t)) \end{aligned}$$

The expression for $\dot{\mathbf{x}}$ and $\hat{\boldsymbol{\theta}} \cdot \hat{\boldsymbol{\phi}} = 0$ immediately provide the kinetic energy

$$T = \frac{M}{2} \dot{\mathbf{x}}^2 = \frac{M}{2} \ell^2 \dot{\theta}^2(t) + \frac{M}{2} \ell^2 \sin^2 \theta(t) \dot{\phi}^2(t)$$

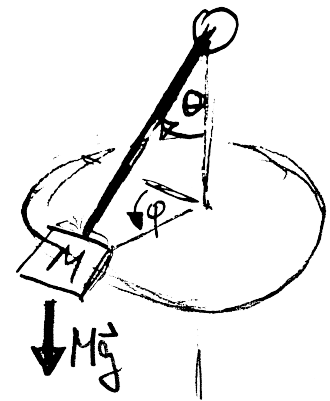


Figure 6.16: Spherical coordinates adopted to describe the motion of a spherical pendulum.

Consequently, the Lagrange function for the spherical pendulum takes the form

$$\mathcal{L}(\theta, \phi, \dot{\theta}, \dot{\phi}) = \frac{M}{2} \ell^2 \dot{\theta}^2 + \frac{M}{2} \ell^2 \sin^2 \theta(t) \dot{\phi}^2(t) + M g \ell \cos \theta(t)$$

We observe that \mathcal{L} does not depend on ϕ . In that case it is advisable to first discuss the EOM for ϕ . It takes the form

$$M \ell^2 \frac{d}{dt} \left(\dot{\phi} \sin^2 \theta(t) \right) = \frac{d}{dt} \frac{\partial \mathcal{L}}{\partial \dot{\phi}} = \frac{\partial \mathcal{L}}{\partial \phi} = 0$$

The derivative of the Lagrange function with respect to ϕ vanishes because \mathcal{L} does not depend on ϕ . Such a coordinate is called a cyclic, and it always implies a conservation law, C . For the spherical pendulum it signifies conservation of the z -component of the angular momentum, and it provides an expression of $\dot{\phi}$ in terms of θ

$$C = \dot{\phi} \sin^2 \theta(t) = \text{const} \quad \Rightarrow \quad \dot{\phi}(t) = \frac{C}{\sin^2 \theta(t)} \quad (6.4.1)$$

where C is proportional to the z -component of the angular momentum.

The general case is summarized in the following definition:

Definition 6.10: Cyclic coordinates

A coordinate q_i is called *cyclic* when the Lagrange function depends only on its time derivative \dot{q}_i , and not on q_i . In that case the associated Euler-Lagrange equation establishes a conservation law,

$$C = \frac{\partial \mathcal{L}}{\partial \dot{q}_i}$$

After all

$$\frac{dC}{dt} = \frac{d}{dt} \frac{\partial \mathcal{L}}{\partial \dot{q}_i} = \frac{\partial \mathcal{L}}{\partial q_i} = 0$$

Remark 6.9. The constant value of C is determined by the initial conditions on \dot{q}_i and on the other coordinates. □

Let us now consider to the other coordinate of the spherical pendulum. The EOM for $\theta(t)$ takes the form

$$\begin{aligned} M \ell^2 \ddot{\theta}(t) &= \frac{d}{dt} \frac{\partial \mathcal{L}}{\partial \dot{\theta}} \\ &= \frac{\partial \mathcal{L}}{\partial \theta} = M \ell^2 \dot{\phi}^2(t) \sin \theta(t) \cos \theta(t) - M g \ell \sin \theta(t) \end{aligned}$$

In this equation the unknown function $\dot{\phi}(t)$ can be eliminated by means of the conservation law, Equation (6.4.1), yielding

$$\ddot{\theta}(t) = \frac{C^2 \cos \theta(t)}{\sin^3 \theta(t)} - \frac{g}{\ell} \sin \theta(t)$$

The resulting EOM can be integrated once by multiplication with $2\dot{\theta}(t)$

$$\begin{aligned} \dot{\theta}^2(t) - \dot{\theta}^2(t_0) &= \int_{t_0}^t dt 2\dot{\theta} \left(\frac{C^2 \cos \theta(t)}{\sin^3 \theta(t)} - \frac{g}{\ell} \sin \theta(t) \right) \\ &= -2 \int_{\theta(t_0)}^{\theta(t)} d\theta \frac{d}{d\theta} \left(-\frac{C^2}{\sin^2 \theta} + \frac{g}{\ell} \cos \theta \right) \end{aligned}$$

The result can be written in the form

$$E = \frac{\dot{\theta}^2}{2} + \Phi_{\text{eff}}(\theta) = \text{const}$$

$$\text{where } \Phi_{\text{eff}}(\theta) = \frac{C^2}{\sin^2 \theta} - \frac{g}{\ell} \cos \theta$$

Again a closed solution for $\theta(t)$ is out of reach. However, $\Phi_{\text{eff}}(\theta)$ can serve as an effective potential for the 1DOF motion of θ with kinetic energy $\dot{\theta}^2/2$. This interpretation of the dynamics provides ready access to a qualitative discussion of the solutions of the EOM based on a phase-space plot.

For $C = 0$ the particle swings in a fixed plane selected by $\phi = \text{const}$. Its motion amounts to that of a mathematical pendulum.

Figure 6.17 shows the effective potential and phase space portraits for different positive values of C . Conservation of angular momentum implies that for $C \neq 0$ the particle can no longer access the region close to its rest position at the lowermost point of the sphere. Rather it always has to go in circles around the bottom of the well, and the sign of C specifies whether it moves clockwise or anti-clockwise. The divergence of the effective potential at $\theta = \pm\pi$ is called *rotation barrier*. It emerges due to a combination of the conservation of energy and angular momentum.

add problem: rotation barrier

Theorem 6.6: Rotation barrier

Let a particle of mass m follow a dynamics where the energy E and a component $L_n = \hat{n} \cdot \mathbf{L}$ of the angular momentum \mathbf{L} are conserved. Then the particle will keep a minimum distance

$$R_{\min} = \frac{L_n}{\sqrt{2m(E - \Phi_{\min})}}$$

from the axis \hat{n} . Here, Φ_{\min} is a lower bound to the potential energy.

Proof. We adopt cylinder coordinates (R, ϕ, z) with a symmetry axis \hat{z} aligned along \hat{n} . Then the kinetic energy and L_n amount to

$$T = \frac{m}{2} (z^2 + R^2 \dot{\phi}^2)$$

$$L_n = m R^2 \dot{\phi}$$

As a consequence, we have

$$E - \Phi_{\min} \geq E - U(R, \phi) = T \geq \frac{m}{2} R^2 \dot{\phi}^2 = \frac{L_n^2}{2m R^2}$$

The bound is obtained by solving this inequality for R . \square

The effective potential has a single minimum for $0 < \theta_c(C) < \pi/2$, and not further extrema. The minimum describes motion where the particle moves at constant height with a constant speed

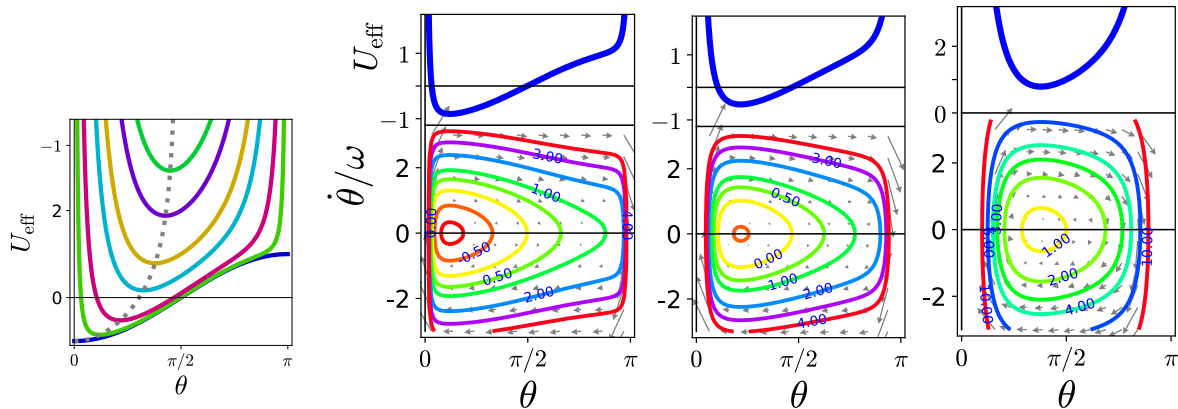


Figure 6.17: The left panel shows the effective potential for the spherical pendulum at parameter values $C^2 \in \{0, 0.01, 0.1, 0.5, 1, 2, 3\}$ from bottom to top. The subsequent panels show phase-space portraits of the motion for $C^2 = 0.01, 0.1, 1, 2, 3$ respectively.

add traces in the (x, y) plane

in a circle. When this orbit is perturbed oscillations are superimposed on the circular motion. In a projection to the plane vertical to the action of gravity, this will lead to trajectories similar to those drawn by a Spirograph, Problem 2.42.

The take-home message of this example is that cyclic variables entail conservation laws of the dynamics. In the very same manner as for the Kepler problem they can be used to eliminate a variable from the EOM of the other coordinates. The additional contributions in the EOMs for the other coordinate(s) are interpreted as part of an effective potential.

6.4.2 Foucault pendulum

6.4.3 Double pendulum

6.5 Dynamics of 2-particle systems

revisit Kepler

6.6 Conservation laws, symmetries, and the Lagrange formalism

6.7 Worked problems: spinning top and running wheel

spinning top

rolling wheel

6.8 Problems

horizontal driven double pendulum

free carousel

stabilizing satellites


Lagrange points

steel can pendulum

6.8.1 Rehearsing Concepts

Problem 6.10. Kitchen pendulum

We consider a pendulum that is built from two straws (length L_1 and L_2), two corks (masses m_1 and m_2), a paper clip, and some Scotch tape (see picture to the right). It is suspended from a shashlik skewer, and its motion is stabilized by means of the spring taken from a discharged ball-pen. Hence, the arms move vertically to the skewer. We denote the angle between the arms as α , and the angle of the right arm with respect to the horizontal as $\theta(t)$.

- Determine the kinetic energy, T , and the potential energy, V , of the pendulum. Argue that T and V can only depend on θ and $\dot{\theta}$, and determine the resulting Lagrangian $\mathcal{L}(\theta, \dot{\theta})$.
 - Determine the EOM of the pendulum.
 - Find the rest positions of the pendulum, and discuss the motion for small deviations from the rest positions. Sketch the according motion in phase space.
 - The EOM becomes considerably more transparent when one selects the center of mass of the corks as reference point. Show that the center of mass lies directly below the fulcrum when the pendulum is at rest.
 - Let ℓ be the distance of the center of mass from the fulcrum, and $\varphi(t)$ be the deflection of their connecting line from the vertical. Determine the Lagrangian $\mathcal{L}(\varphi, \dot{\varphi})$ and the resulting EOM for $\varphi(t)$.
-  f) Do you see how the equations for $\dot{\theta}(t)$ and $\ddot{\varphi}(t)$ are related?

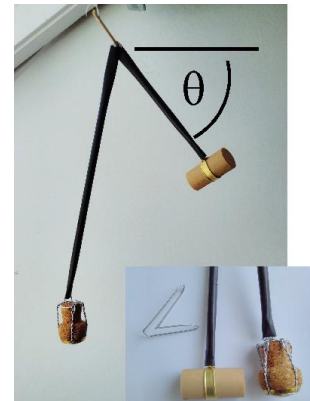


Figure 6.18: Setup of the kitchen pendulum.

6.8.2 Mathematical Foundation

Problem 6.11. Shortest path on a sphere

We describe the position on the surface of a three-dimensional sphere by the angle θ with its “North pole”, and the azimuthal angle ϕ in the horizontal plane. A trajectory on the sphere with radius R can then be specified as $\mathbf{q}(t) = R \hat{\mathbf{r}}(\theta(t), \phi(t))$, or alternatively by $\theta(\phi)$ or $\phi(\theta)$. We will now derive conditions for a path of extremal length on the sphere.

- Without restriction of generality we restrict our discussion to spheres with unit radius, $R = 1$. Why is this admissible?

- b) Show that the length of the path from $(\theta(t_i), \phi(t_i)) = (\theta_i, \phi_i)$ to $(\theta(t_e), \phi(t_e)) = (\theta_e, \phi_e)$ amounts to

$$\begin{aligned} L &= \int_{t_i}^{t_e} dt \left| \dot{\mathbf{r}}(\theta(t), \phi(t)) \right| = \int_{\phi_i}^{\phi_e} d\phi \sqrt{\sin^2 \theta(\phi) + \left(\frac{d\theta(\phi)}{d\phi} \right)^2} \\ &= \int_{\theta_i}^{\theta_e} d\theta \sqrt{1 + \sin^2 \theta \left(\frac{d\phi(\theta)}{d\theta} \right)^2} \end{aligned}$$

Under which conditions do the expressions apply? Why and when do they provide the same length?

- c) A necessary condition for the extremality of L is that the variation δL vanishes for the integrals that have been defined in (b). Introduce the variation $\theta(\phi) + \varepsilon \delta\theta(\phi)$ into the second representation of the length (i.e., the one involving an integral over ϕ), calculate δL , and determine the resulting differential equation for paths $\theta(\phi)$ of extremal length.
- d) Repeat the same steps for the variation $\phi(\theta) + \delta\phi(\theta)$ and the representation of the length in terms of $\phi(\theta)$. Determine the resulting differential equation for paths $\phi(\theta)$ of extremal length. Which derivation is simpler? How could you have seen this *before* performing the calculations?
- e) The result of (d) can be integrated once. Show that this results in the following first order differential equation

$$\frac{d\phi}{d\theta} = \frac{\cos \alpha}{\sin \theta} \left[\sin^2 \alpha - \cos^2 \theta \right]^{-1/2}.$$

where $\sin \alpha$ is an integration constant.

- f) Verify that the following function is a solution of the differential equation

$$\phi(\theta) = \phi_0 - \arcsin \frac{\cos \alpha \cos \theta}{\sin \alpha \sin \theta}.$$

Hint: Express $\sin(\phi - \phi_0)$ as a function of θ . Take the θ derivative of both sides of the equation. Subsequently, you can determine $\phi'(\theta)$ by eliminating $\cos(\phi - \phi_0)$ by means of the known expression for $\sin(\phi - \phi_0)$.

- g) Show that all the coordinates

$$\mathbf{q}(\theta) = (\sin \theta \cos \phi(\theta), \sin \theta \sin \phi(\theta), \cos \theta)$$

of the trajectory obtained in (f) are orthogonal to the vector $(0, \sin \alpha, \cos \alpha)$.

Then: How does the path look like on the sphere?

- h) The path from the initial point to the final point on the sphere is not unique! One of the solutions is the shortest path on the sphere. What type of an extremum does the other path represent?

- ★ i) Consider the following ODE for a path on the sphere

$$\dot{\mathbf{r}}(\theta(t), \phi(t)) = (\hat{\mathbf{q}}_1 \times \hat{\mathbf{q}}_2) \times \hat{\mathbf{r}}(\theta(t), \phi(t))$$

where $\hat{\mathbf{q}}_1$ and $\hat{\mathbf{q}}_2$ are two distinct points on the sphere. Show that for the initial condition $\hat{\mathbf{q}}_1$ the trajectory will proceed through $\hat{\mathbf{q}}_2$.

How long does it take to arrive at $\hat{\mathbf{q}}_2$?

Does the trajectory represent an extremal path on the sphere?

Under which conditions would it be a path of minimal length?

add torus and cone

Problem 6.12. 1D dynamical systems with pitchfork and saddle-node bifurcations

We consider the dynamical systems

$$\dot{x}_a(t) = a + x^2(t) \quad (6.8.1)$$

We will analyze now how the solutions $x(t)$ change upon varying the parameter $a \in \mathbb{R}$.

- With no loss of generality we will assume that $t_0 = 0$ and $x_0 = x(t_0) = 1$. Why is this admissible?
Hint: 1. How would the solutions differ when one chooses $t_0 = 1$ rather than $t_0 = 0$?
2. Consider the evolution of $x(t)/x_0^2$ with a suitable change of the time unit and the parameter a .
- With no loss of generality we will assume that $a \in \{-1, 0, 1\}$. Why is this admissible?
Hint: For $a \neq 0$ you may divide the ODE by $\sqrt{a^2} = (\sqrt{|a|})^2$.
- Solve the differential equation by separation of variables and partial fraction decomposition.
- Plot the solutions $x_a(t)$ for $a = -1$, $a = 0$, and $a = 1$.
What does this plot tell about the solutions for general t_0 , x_0 , and a ?
- Determine the fixed points of Equation (6.8.1) and plot the bifurcation diagram.
Can you see how the structure of the bifurcation diagram fits with the explicit solutions obtained in d)?
- Repeat the analysis for the system

$$\dot{x}(t) = a x(t) + x^3(t)$$

Bibliography

- Archimedes, 1878, in *Pappi Alexandrini Collectionis, Book VIII, c. AD 340*, edited by F. O. Hultsch (Apud Weidmannos, Berlin), p. 1060, cited following https://commons.wikimedia.org/wiki/File:Archimedes_lever,_vector_format.svg.
- Arnol'd, V. I., 1992, *Ordinary Differential Equations* (Springer, Berlin).
- Epstein, L. C., 2009, *Thinking Physics, Understandable Practical Reality* (Insight Press, San Francisco).
- Finney, G. A., 2000, *American Journal of Physics* **68**, 223–227.
- Gale, D. S., 1970, *American Journal of Physics* **38**, 1475.
- Gommes, C. J., 2010, *Am. J. Phys.* **78**, 236.
- Großmann, S., 2012, *Mathematischer Einführungskurs für die Physik* (Springer), very clear introduction of the mathematical concepts for physics students., URL <https://doi.org/10.1007/978-3-8348-8347-6>.
- Harte, J., 1988, *Consider a Spherical Cow: A Course in Environmental Problem Solving* (University Science Books, Melville, NY), ISBN 978-0-935702-58-3, URL <https://uscibooks.aip.org/books/consider-a-spherical-cow-a-course-in-environmental-problem-solving/>.
- Kagan, D., L. Buchholtz, and L. Klein, 1995, *Phys.Teach.* **33**, 150.
- Lueger, O., 1926–1931, *Luegers Lexikon der gesamten Technik und ihrer Hilfswissenschaften* (Dt. Verl.-Anst., Stuttgart), URL <https://digitalesammlungen.uni-weimar.de/viewer/resolver?urn=urn:nbn:de:gbv:wim2-g-3163268>.
- Mahajan, S., 2010, *Street-Fighting Mathematics: The Art of Educated Guessing and Opportunistic Problem Solving* (MIT press, Cambridge, MA), ISBN 9780262514293, cCed full text available as <https://www.dropbox.com/s/z1ibh5txrs91lia/7728.pdf?dl=1>, URL <https://mitpress.mit.edu/books/street-fighting-mathematics>.
- Morin, D., 2007, *Introduction to Classical Mechanics* (Cambridge), comprehensive introduction with a lot of exercises—many of

them with worked solutions. The present lectures cover the Chapters 1–8 of the book. I warmly recommend to study Chapters 1 and 6., URL <https://scholar.harvard.edu/david-morin/classical-mechanics>.

Morin, D., 2014, *Problems and Solutions in Introductory Mechanics* (CreateSpace), a more elementary introduction with a lot of solved exercises self-published at Amazon. Some Chapters can also be downloaded from the autor's home page, URL <https://scholar.harvard.edu/david-morin/mechanics-problem-book>.

Murray, J., 2002, *Mathematical Biology* (Springer).

Nordling, C., and J. Österman, 2006, *Physics Handbook for Science and Engineering* (Studentlitteratur, Lund), 8 edition, ISBN 91-44-04453-4, quoted after [Wikipedia's List of humorous units of measurement](#), accessed on 5 May 2020.

Purcell, E. M., 1977, *American Journal of Physics* **45**(3).

Seifert, H. S., M. W. Mills, and M. Summerfield, 1947, *American Journal of Physics* **15**(3), 255.

Sommerfeld, A., 1994, *Mechanik*, volume 1 of *Vorlesungen über theoretische Physik* (Harri Deutsch, Thun, Frankfurt/M.).

Zee, A., 2020, *Fly by Night Physics: How Physicists Use the Backs of Envelopes* (Princeton UP, Princeton, NJ), ISBN 9780691182544, errors and addenda available at <https://www.kitp.ucsb.edu/zee/books/fly-by-night-physics>, URL <https://press.princeton.edu/books/hardcover/9780691182544/fly-by-night-physics>.

Index

- action, 166
- algorithm
 - Euler Lagrange EOM, 171
 - phase space plot, 176
- axiom
 - principle of least action, 166
- bifurcation
 - pitchfork, 180
 - saddle node
 - soap film, 173
 - saddle-node, 185
- centrifugal governor, 180
- coordinates
 - polar
 - mathematical pendulum, 174
 - spherical
 - spherical pendulum, 187
- cyclic variables, 188
- cylindrical coordinates
 - unit vectors, 182
- d'Alembert's principle, 170
- driven pendulum, 169
- equation of motion
 - centrifugal governor, 180
 - mathematical pendulum, 174
 - pearl on rotating ring, 177
 - spherical pendulum, 187
- Fermat's principle, 172
- generalized coordinates, 162
- heterocline, 175
- homocline, 175
- Lagrange
 - cyclic variable, 188
- Lagrange formalism
 - and dissipation, 180
- Lagrangian, 166
 - Cartesian coordinates, 166
 - in generalized coordinates, 171
- mathematical pendulum
 - Lagrange coordinates, 162
 - Lagrange EOM, 174
- pearl on rotating ring, 185
 - Lagrange EOM, 177
- pendulum
 - driven, 169
- Phase Diagram, 184
- pitchfork bifurcation, 180
- polar coordinates
 - unit vectors, 163
- principle
 - d'Alembert's, 170
- principle of least action, 166
- rollercoaster trail, 169
- Rotation barrier, 189
- rotation barrier, 189
- saddle-node bifurcation, 185
- Snellius' law, 172
- Soap film, 173
- spherical coordinates
 - unit vectors, 177, 185
- spherical pendulum
 - Lagrange EOM, 187

- variation of a function, [165](#)
- variational calculus
 - Fermat's principle, [172](#)
 - shortest path
 - in plane, [167](#)
 - on catenoid, [168](#)
 - on cylinder, [168](#)
 - on sphere, [191](#)
 - soap film, [173](#)